Agricultural and Forest Meteorology 187 (2014) 46–61

Contents lists available at ScienceDirect

Agricultural and Forest Meteorology

journal homepage: www.elsevier.com/locate/agrformet

Multi-site evaluation of terrestrial evaporation models using FLUXNET data

A. Ershadi[a,*], M.F. McCabe[b], J.P. Evans[c,d], N.W. Chaney[e], E.F. Wood[e]

[a] School of Civil & Environmental Engineering, University of NSW, Sydney, NSW, Australia
[b] Water Desalination and Reuse Centre, King Abdullah University of Science and Technology (KAUST), Jeddah, Saudi Arabia
[c] ARC Centre of Excellence for Climate Systems Science, University of NSW, Sydney, Australia
[d] Climate Change Research Centre, University of NSW, Sydney, Australia
[e] Department of Civil and Environmental Engineering, Princeton University, Princeton, NJ, USA

ARTICLE INFO

Article history:
Received 3 March 2013
Received in revised form 5 October 2013
Accepted 23 November 2013

Keywords:
Multi-model intercomparison
Latent heat flux
Energy balance
Penman–Monteith
Advection-aridity
Priestley–Taylor

ABSTRACT

We evaluated the performance of four commonly applied land surface evaporation models using a high-quality dataset of selected FLUXNET towers. The models that were examined include an energy balance approach (Surface Energy Balance System; SEBS), a combination-type technique (single-source Penman–Monteith; PM), a complementary method (advection-aridity; AA) and a radiation based approach (modified Priestley–Taylor; PT-JPL). Twenty FLUXNET towers were selected based upon satisfying stringent forcing data requirements and representing a wide range of biomes. These towers encompassed a number of grassland, cropland, shrubland, evergreen needleleaf forest and deciduous broadleaf forest sites. Based on the mean value of the Nash–Sutcliffe efficiency (*NSE*) and the root mean squared difference (*RMSD*), the order of overall performance of the models from best to worst were: ensemble mean of models (0.61, 64), PT-JPL (0.59, 66), SEBS (0.42, 84), PM (0.26, 105) and AA (0.18, 105) [statistics stated as (*NSE*, *RMSD* in $W\,m^{-2}$)]. Although PT-JPL uses a relatively simple and largely empirical formulation of the evaporative process, the technique showed improved performance compared to PM, possibly due to its partitioning of total evaporation (canopy transpiration, soil evaporation, wet canopy evaporation) and lower uncertainties in the required forcing data. The SEBS model showed low performance over tall and heterogeneous canopies, which was likely a consequence of the effects of the roughness sub-layer parameterization employed in this scheme. However, SEBS performed well overall. Relative to PT-JPL and SEBS, the PM and AA showed low performance over the majority of sites, due to their sensitivity to the parameterization of resistances. Importantly, it should be noted that no single model was consistently best across all biomes. Indeed, this outcome highlights the need for further evaluation of each model's structure and parameterizations to identify sensitivities and their appropriate application to different surface types and conditions. It is expected that the results of this study can be used to inform decisions regarding model choice for water resources and agricultural management, as well as providing insight into model selection for global flux monitoring efforts.

1. Introduction

Reliable estimates of evaporation (E) are required for the accurate representation of mass and energy exchanges at the land surface. In hydrological and water resource studies, an evaporation model is required to characterize the exchange of moisture between the surface and the overlying atmosphere. Not surprisingly, the choice of model can have considerable impact on water resource planning and decision support across a range of temporal and spatial scales. Improved understanding of the influence of model choice on flux estimation is required in order to better characterize the fidelity of these simulations, particularly in light of an increasing number of regional and global scale efforts to produce land surface heat flux data products (Jiménez et al., 2011; Mueller et al., 2013).

A number of models have been developed for the estimation of either the reference, potential or actual values of evaporation (see reviews of Kalma et al., 2008 and Wang and Dickinson, 2012). The reference evaporation is defined as the evaporation from a hypothetical, well-watered 'reference' crop (Allen, 2000), while potential evaporation is the maximum evaporation for a given surface if moisture is not limiting (Penman, 1948; Irmak and Haman, 2003). Estimation of the reference and potential evaporation is

* Corresponding author. Tel.: +61 403053522.
E-mail addresses: a.ershadi@studnet.unsw.edu.au (A. Ershadi), matthew.mccabe@kaust.edu.sa (M.F. McCabe), jason.evans@unsw.edu.au (J.P. Evans), nchaney@princeton.edu (N.W. Chaney), efwood@princeton.edu (E.F. Wood).

0168-1923/$ – see front matter © 2013 Elsevier B.V. All rights reserved.
http://dx.doi.org/10.1016/j.agrformet.2013.11.008

usually based on meteorological data using relatively straightforward techniques (Penman, 1948; Doorenbos and Pruitt, 1975; Allen et al., 1998). On the other hand, actual evaporation is the evaporation from the land surface, either wet or moisture "stressed", which requires consideration of resistance schemes to describe the environmental constraints on evaporative water loss (Brutsaert, 1982; Rana and Katerji, 2000). As a result, scaling of the potential and reference evaporation to actual values is often problematic due to the difficulties in parameterization of the soil–plant–atmosphere interactions and other bio-physiological constraints. These difficulties are especially pronounced in arid and semi-arid environments with limitations on water availability.

The majority of models used in the estimation of the actual evaporation can be categorized broadly into energy balance approaches, combination-type techniques, complementary methods or radiation based schemes (Brutsaert, 1982, 2005). The central concept behind the formulation of these models is the transfer of sensible heat and water vapour from the land surface to the overlying atmosphere: a process that is well described by the Monin–Obukhov similarity theory (Monin and Obukhov, 1945; Brutsaert, 1982). In energy balance approaches such as the Surface Energy Balance System (SEBS) (Su, 2002), the focus is on the transfer of sensible heat flux (H), with the actual evaporation (or the latent heat flux, λE) estimated as the residual term in the general energy balance equation ($\lambda E = R_n - G - H$). λE is actual evaporation in W m^{-2} (used also to refer to the related term E in this manuscript), λ is the latent heat of vaporization (=2.43 $\times$ 10^6 J kg^{-1}), E is the volume of water evaporated, R_n is net radiation (W m^{-2}) and G is ground heat flux (W m^{-2}). Combination-type models of actual evaporation, conceptualized well by the ubiquitous Penman–Monteith approach (Monteith, 1965), are based on the similarity in heat and water vapour transfer, as defined by the Bowen ratio concept (Bowen, 1926). The complementary approach to actual evaporation, as described here by the advection-aridity method (Brutsaert and Stricker, 1979), is based on the complementary feedback between actual and potential evaporation. This complementary mechanism suggests that if actual evaporation decreases below its true potential value, the amount of energy not used by evaporation becomes available as sensible heat. Finally, radiation based approaches such as the Priestley–Taylor method (Priestley and Taylor, 1972) describe a simplified form of the Penman–Monteith combination model, allowing flux estimation with a minimum of meteorological and radiation information. More detailed descriptions and explanations of these model classes are provided in Section 2.2.

All of the models described above vary in structural complexity, parameterization and the level of data required to run them. Hence, their performance in estimating actual evaporation is expected to differ over various land surface types and conditions. Furthermore, models are expected to present different behaviour when dealing with the combined uncertainties of input data and parameterizations (Massman and Lee, 2002; McCabe et al., 2005; Richardson et al., 2006; Williams et al., 2009; Ershadi et al., 2013b). Consequently, finding an appropriate model for a given land surface has motivated a number of model intercomparison studies. The majority of such studies have focused on an evaluation of the reference or potential evaporation (Trambouze et al., 1998; Xu and Singh, 2002; Lu et al., 2005; Bormann, 2011; Fisher et al., 2011; Xystrakis and Matzarakis, 2011), while others have examined actual evaporation models. For instance, Crago and Brutsaert (1992) evaluated several evaporation models, including the advection-aridity and Penman–Monteith schemes, over the First ISCLCP Field Experiment (FIFE) in Kansas and found that the advection-aridity model produced acceptable results under generally moist conditions. Sumner and Jacobs (2005) evaluated the Penman–Monteith and Priestley–Taylor methods against eddy covariance measurements of evaporation over a natural pasture site in Florida and found that the Priestley–Taylor method, with a calibrated alpha coefficient (α_{PT}), provided the best estimates. Cleugh et al. (2007) compared energy balance and combination methods over forest and savannah sites in Australia. The authors found that while the Penman–Monteith combination technique provided an adequate estimate of the observed evaporation (R^2 = 0.74, $RMSD$ = 27 W m^{-2}), the energy balance approach did not, due to its sensitivity to uncertainties in the land surface temperature measurements. More recently, Vinukollu et al. (2011b) evaluated an energy balance, Penman–Monteith and Priestley–Taylor models over 16 FLUXNET towers and concluded that the Priestley–Taylor performed the best out of these competing schemes. Liu et al. (2013) compared evaporation estimates from a number of models, including the Penman–Monteith model variant developed by Mu et al. (2011) (PM–Mu) and a Priestley–Taylor based model developed by Miralles et al. (2011) (Global Land-surface Evaporation: the Amsterdam Methodology – GLEAM) over the Mongolian Plateau. They found that at the tower scale, the seasonal variability of the models matched well, except for the winter months, when PM–Mu overestimated E.

Many of these evaluation and intercomparison studies have provided a solid assessment of a number of modelling schemes at particular locations. However, a basis from which to make an informed model choice remains missing. In particular, selection of the best candidate evaporation model for global applications (Jiménez et al., 2011; Mueller et al., 2011) is not supported in any of the current model intercomparison contributions. This is due to a number of reasons, including:

- **Spatial and temporal extent**: most previous studies have compared models over single (or a few) locations and for relatively short time periods with limited variability in the land surface type and condition. For example, the model evaluations by Crago and Brutsaert (1992), Stannard (1993), Trambouze et al. (1998) and Sumner and Jacobs (2005) were only performed over one location for 42 days, 55 days, 2 months and 10 months respectively;
- **Reduced range of models examined**: the most comprehensive studies were those undertaken by Stannard (1993) and Vinukollu et al. (2011b), where comparisons of energy balance, combination and radiation based methods were undertaken;
- **Low temporal resolution**: With the exception of Sumner and Jacobs (2005), Pauwels and Samson (2006) and Shi et al. (2008), the majority of previous studies have used daily (Crago and Brutsaert, 1992; Xu and Chen, 2005; Schneider et al., 2007) or monthly (Vinukollu et al., 2011b) temporal resolutions. Aggregation of input meteorological forcing to coarser temporal resolutions can greatly affect the simulation results, either positively by reducing the uncertainty in input data, or negatively by increasing the temporal mismatch between different input variables (and parameters). For example, one reason behind the poor performance of the energy balance approach in the Cleugh et al. (2007) study was the use of aggregated tower based meteorological data with 16 days aggregated Moderate Resolution Imaging Spectroradiometer (MODIS) land surface temperature;
- **Prior model calibration**: in a number of studies (e.g. Sumner and Jacobs, 2005; Shi et al., 2008), model parameters were calibrated locally, limiting the utility of the studied model to those specific locations or areas with similar meteorological and land surface conditions;
- **Model parameterization**: often, the vegetation parameters (e.g. leaf area index) required for parameterization of aerodynamic and surface resistances were assumed constant due to the limitations in the field or remote sensing observations. As a result, the dynamics of vegetation growth and its effects on evaporation were overlooked. The incorporation of vegetation dynamics can significantly improve modelling performance, particularly in

the models that are more sensitive to the parameterization of aerodynamic and surface resistances (Cleugh et al., 2007; Tang et al., 2011).

In the present study, the objective is to understand and evaluate the performance of a number of the most commonly utilised models of actual evaporation across a variety of land surface types and conditions. This effort is achieved by using a collection of high-quality tower based data, collected over an extensive observation period that enables an adequate representation of meteorological variability.

The main research questions of this study include:

- What is the performance of the selected evaporation models and their ensemble mean over different biomes and surface conditions?
- What is the performance of the selected evaporation models over different seasons?
- Do more complex and data-intensive models perform better than simpler schemes?
- Do violation of a model's underlying theoretical assumptions effect simulation performance? (e.g. impacts of footprint homogeneity, stability conditions)
- What are the main sources of uncertainty in evaporation estimation using the selected models?

2. Data and methodology

2.1. Forcing data

One of the principal limitations in the evaluation of evaporation models is the availability of accurate and descriptive input forcing data. The FLUXNET project (Baldocchi et al., 2001; Agarwal et al., 2010) provides a high-quality, community based globally distributed dataset of surface heat fluxes and meteorological data, making them an appropriate source for model evaluation. In this study, 20 eddy covariance FLUXNET towers were selected across a range of representative biomes that included grassland (GRA), cropland (CRO), shrubland (SHR), evergreen needleleaf forest (ENF) and deciduous broadleaf forest (DBF).

2.1.1. Tower based in-situ measurements

Four towers were selected for each biome type based on a number of criteria, including: (a) variations in vegetation height; (b) being spatially distributed; (c) quality controlled; (d) having extensive period of data with minimal gaps; and (e) the availability of all required input data for simulation using the different models in this study. While there are approximately 545 towers within the FLUXNET database (http://fluxnet.ornl.gov/site_status), open access to the data and the range of input variables required for the comprehensive assessment of the evaporation models used in this study significantly limits the choice of towers. In particular, soil moisture (required for surface resistance specification in the Penman–Monteith model) and longwave upward radiation data (used in the calculation of the land surface temperature for the SEBS model) were only available at a reduced number of sites. Likewise, the start of the selected tower records was limited to the year 2000, when remote sensing data required for the resistance parameterization was available (see Section 2.1.2). The 20 selected towers provide sufficient data to capture a range of land surface conditions at each of the individual sites. The Santa Rita Creosote tower has the shortest data span used here (1.5 years), while the US Mead towers provided the longest (10 years) period of data. The average length of record across the towers is 5 years.

All tower data were filtered for daytime only measurements to avoid having to deal with negative net radiation and nighttime condensation, since these are conditions that are not well represented by any of the models. Daytime is defined to be when the shortwave downward radiation at the tower was greater than 20 W m^{-2}. This criterion is rather strict, but selected to also filter out the times when early morning and late afternoon transitions in the atmospheric boundary layer occur. The physics of such conditions are not well captured by any of the models and would add uncertainties to the estimated *E*. Data were also filtered for a number of meteorological and quality control constraints to ensure the highest-quality forcing data set. These include rain events, frozen periods (when the air or land surface temperature are less than or equal to zero), negative observed turbulent fluxes, gap-filled records and low quality flagged FLUXNET data. Overall, more than 100 site-years of data, or approximately 500,000 filtered records, were selected for each of the four models. Characteristics of the selected eddy covariance towers are provided in Table 1. A map of the spatially distributed tower locations is presented in Fig. 1.

The level of data pre-processing used in this study varies depending on the data source (refer to Column *L* of Table 1). Level 3 data are the quality controlled and gap-filled data obtained from fluxdata.org. Level 2 data are obtained from ameriflux.ornl.gov and no gap-filling or quality control is applied to those data. Although the AmeriFlux dataset provides Level 3 data, only Level 2 data are used here, since in Level 3 the longwave upward radiation is missing. Data from fluxdata.org are provided at half-hourly temporal resolution, while those from ameriflux.ornl.gov are at an hourly temporal resolution. Both temporal resolutions are used directly in the modelling intercomparison without any aggregation.

The data used from the towers include air temperature, wind speed, humidity, net radiation, ground heat flux and soil moisture. The land surface temperature was derived from tower observations of longwave upward radiation by inverting the Stefan–Boltzmann equation, with emissivity calculated from the Normalized Difference Vegetation Index (*NDVI*) using the methodology of Sobrino et al. (2004).

2.1.2. Remote sensing based measurements

Time series of *NDVI* was extracted from the MOD13Q1 product (Solano et al., 2010) at each tower location. The MOD13Q1 data are derived from the MODIS sensor onboard the Terra satellite and provide 250 m spatial and 16 days temporal resolution. Data were obtained from the Simple Object Access Protocol (SOAP) web services of the Oak Ridge National Laboratory (ORNL) MODIS Land Product Subsets (http://daac.ornl.gov/MODIS/). The 16-day gaps between successive *NDVI* records were filled using linear interpolation. The leaf area index and fractional vegetation cover (required for aerodynamic and surface resistance parameterizations) were calculated from the *NDVI* data using the methodology of Ross (1976) and Jiménez-Muñoz et al. (2009) respectively. All evaporation models use the same values of leaf area index and fractional vegetation cover for their parameterization.

2.2. Model descriptions

2.2.1. The Surface Energy Balance System (SEBS): an energy budget approach

The SEBS model of Su (2002) is a physically based model that uses a combination of remote sensing and in-situ observations to derive the land surface variables, radiative heat fluxes and roughness parameters required for calculating actual evaporation. The main inputs to the SEBS model include land surface temperature, vegetation height and density, air temperature, humidity and wind speed, along with surface radiation components. When the measurement height of meteorological variables is in the

Table 1
Selected flux towers and their attributes. z_g is the site elevation (above sea level) in m, z_m is tower height in m, h_c is the canopy height in m, Y is the number of years of data and L is the processing level of data.

	ID	Name	Country	Lat	Lon	z_g	z_m	h_c	Y	L	Reference
Grasslands											
G1	PT-Mi2	Mitra IV Tojal	Portugal	38.5	−8.0	190	2.5	0.05	2	3	Gilmanov et al. (2007)
G2	US-Aud	Audubon Research Ranch	USA	31.6	−110.5	1469	4	0.15	4	3	Horn and Schulz (2011)
G3	US-Goo	Goodwin Creek	USA	34.3	−89.9	87	4	0.3	4	3	Hollinger et al. (2010)
G4	US-Fpe	Fort Peck	USA	48.3	−105.1	634	3.5	0.3	4	3	Horn and Schulz (2011)
Croplands											
C1	US-ARM	ARM SGP – Lamont	USA	36.6	−97.5	314	60	0.5	4	3	Lokupitiya et al. (2009)
C2	US-Ne3	Mead – rainfed	USA	41.2	−96.4	363	6	2.5	10	3	Richardson et al. (2006)
C3	US-Ne1	Mead – irrigated	USA	41.2	−96.5	361	6	3	10	3	Richardson et al. (2006)
C4	US-Bo1	Bondville	USA	40.0	−88.3	219	10	3	7	3	Hollinger et al. (2010)
Shrubland/Woody Savannas											
S1	US-SRc	Santa Rita Creosote	USA	31.9	−110.8	991	4.25	1.7	1.5	2	Cavanaugh et al. (2011)
S2	US-SRM	Santa Rita Mesquite	USA	31.8	−110.9	1116	6.4	2.5	7	2	Cavanaugh et al. (2011)
S3	BW-Ma1	Maun-Mopane Woodland	Botswana	−19.9	23.6	950	13.5	8	2	3	Veenendaal et al. (2004)
S4	AU-How	Howard Springs	Australia	−12.5	131.2	38	23	15	5	3	Hutley et al. (2005)
Evergreen needleleaf forest											
E1	NL-Loo	Loobos	Netherlands	52.2	5.7	25	52	15.9	5	3	Sulkava et al. (2011)
E2	US-Fuf	Flagstaff -Unmanaged Forest	USA	35.1	−111.8	2180	23	18	6	2	Román et al. (2009)
E3	DE-Tha	Anchor St. Tharandt – old spruce	Germany	51.0	13.6	380	42	30	2	3	Delpierre et al. (2009)
E4	US-Wrc	Wind River Crane Site	USA	45.8	−122.0	371	85	56.3	9	2	Wharton et al. (2009)
Deciduous broadleaf forest											
D1	US-MOz	Missouri Ozark Site	USA	38.7	−92.2	219	30	24.2	5	2	Hollinger et al. (2010)
D2	US-WCr	Willow Creek	USA	45.8	−90.1	520	30	24.3	5	3	Curtis et al. (2002)
D3	US-MMS	Morgan Monroe State Forest	USA	39.3	−86.4	275	48	27	6	2	Dragoni et al. (2011)
D4	DE-Hai	Hainich	Germany	51.1	10.5	430	43.5	33	3	3	Rebmann et al. (2005)

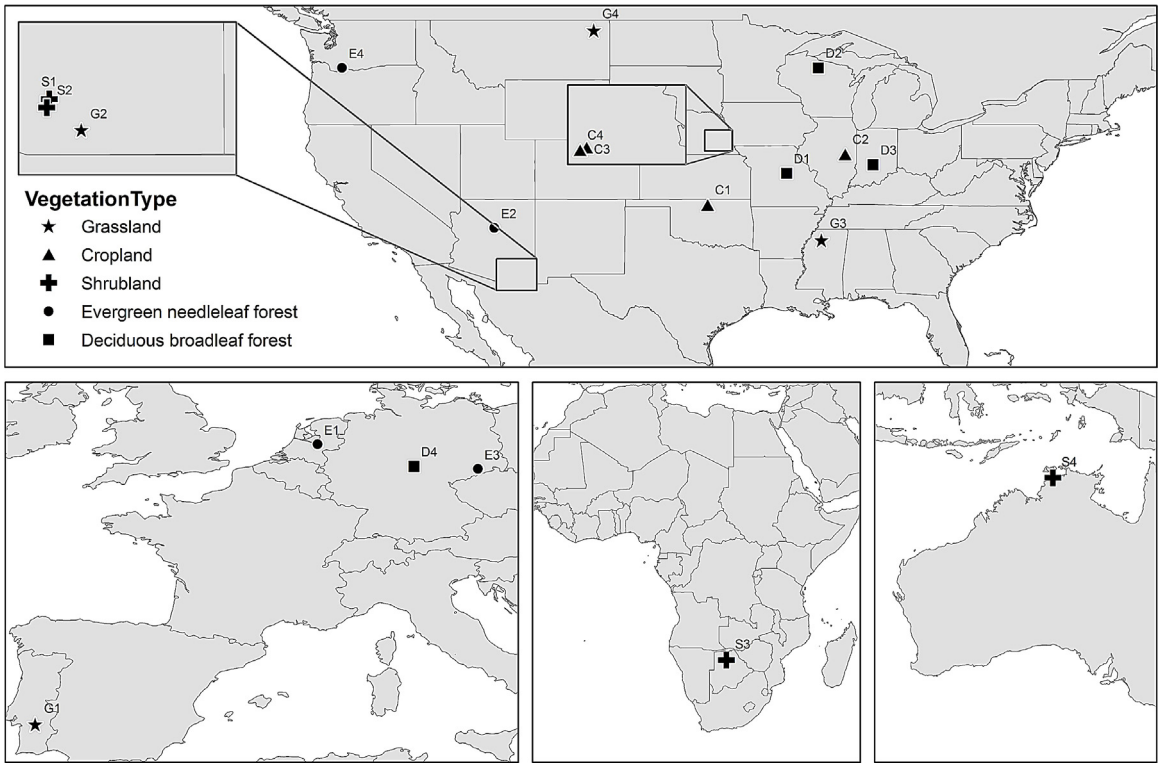

Fig. 1. Location of the eddy covariance towers used to provide forcing and validation data in this study.

atmospheric surface layer, the SEBS model uses the Monin–Obukhov similarity theory (MOST) equations (Monin and Obukhov, 1945). When the measurement height is within the mixed layer of the atmosphere, SEBS uses the Bulk Atmospheric Similarity Theory (BAST) (Brutsaert, 1999). However, in the majority of cases, MOST equations are used unless the roughness of the surface is high or the height of the atmospheric surface layer is low. The MOST equations used in SEBS include stability-dependent flux-gradient functions for momentum and heat transfer, as described below:

$$u = \frac{u_*}{\kappa}\left[\ln\left(\frac{z-d_0}{z_{0m}}\right) - \Psi_m\left(\frac{z-d_0}{L}\right) + \Psi_m\left(\frac{z_{0m}}{L}\right)\right] \quad (1)$$

$$\theta_s - \theta_a = \frac{H}{\kappa u_* \rho c_p}\left[\ln\left(\frac{z-d_0}{z_{0h}}\right) - \Psi_h\left(\frac{z-d_0}{L}\right) + \Psi_h\left(\frac{z_{0h}}{L}\right)\right] \quad (2)$$

where z is the reference height above the land surface for measurement of the meteorological variables (m), u is wind speed ($m\,s^{-1}$), u_* is the friction velocity ($m\,s^{-1}$), ρ is the density of the air ($kg\,m^{-3}$), c_p is specific heat capacity of air at constant pressure ($J\,kg^{-1}\,K^{-1}$), $\kappa = 0.41$ is the von Karman's constant (–), θ_s is the potential land surface temperature (K), θ_a is the potential air temperature (K) at height z, H is the sensible heat flux ($W\,m^{-2}$), d_0 is the zero-plane displacement height (m), z_{0m} is the roughness height for momentum transfer (m), z_{0h} is the roughness height for heat transfer (m) and Ψ_m and Ψ_h are the stability correction functions for momentum and heat transfer. L is the Obukhov length (m) defined as:

$$L = -\frac{\rho c_p u_*^3 \theta_v}{\kappa g H} \tag{3}$$

with g the acceleration due to gravity ($m\,s^{-2}$) and θ_v the atmospheric virtual potential temperature (K).

For atmospheric stability corrections in the atmospheric surface layer, the functions proposed by Beljaars and Holtslag (1991) are used for stable conditions and the functions proposed by Brutsaert (2005) are used for unstable conditions. The roughness length for momentum and heat transfer (z_{0m} and z_{0h}) are estimated in SEBS using the methodology developed by Su et al. (2001), which employs vegetation phenology, air temperature and wind speed.

SEBS uses a correcting method to scale the MOST derived sensible heat flux between hypothetical dry and wet limits based on the relative evaporation concept. Finally, this scaled sensible heat flux can be used to calculate the latent heat flux (λE) as a residual term in the general energy balance equation as $\lambda E = R_n - G - H$. Further details on the SEBS model description are provided by Su (2002) and Su et al. (2005).

2.2.2. Penman–Monteith (PM): a combination-type technique

The Penman–Monteith model (PM) incorporates heat and water vapour mass transfer principles and is therefore known as a combination equation. The Penman equation (Penman, 1948) was developed originally for the estimation of potential evaporation from open water and saturated land surfaces, but was later modified by Monteith (1965) with the introduction of a canopy resistance term to describe the influence of plants on the water vapour transfer through the roots, stems and leaves of the plants. The Penman–Monteith model of actual evaporation can be formulated following Brutsaert (2005):

$$\lambda E = \frac{\Delta (R_n - G) + \rho c_p (e^* - e)/r_a}{\Delta + \gamma \left(1 + r_s/r_a\right)} \tag{4}$$

where Δ ($Pa\,K^{-1}$) is the slope of the saturation water vapour pressure curve $e^* = e^*(T_a)$ at the air temperature T_a, γ is the psychrometric constant defined as $\gamma = c_p p/(0.622\lambda)$ in $Pa\,K^{-1}$, $e^* - e$ is the vapour pressure deficit in Pa, e^* is saturation vapour pressure of the air (Pa), e is actual vapour pressure of the air (Pa) and r_a and r_s are aerodynamic and surface resistances ($s\,m^{-1}$). The aerodynamic resistance r_a was estimated using an equation suggested by Thom (1975) as following:

$$r_a = \frac{1}{\kappa^2 u_a}\left[\ln\left(\frac{z-d_0}{z_{0m}}\right)\ln\left(\frac{z-d_0}{z_{0v}}\right)\right] \tag{5}$$

where z_{0v} is the roughness height for water vapour transfer (m). Following Brutsaert (2005) we assumed $z_{0v} = z_{0h}$ with z_{0h} and z_{0m} calculated using the Su et al. (2001) method, as employed in the SEBS model. For estimation of the surface resistance, the Jarvis scheme of Jacquemin and Noilhan (1990) is used as following:

$$r_s = \frac{r_s^{\min}}{LAI \cdot F_1 \cdot F_2 \cdot F_3 \cdot F_4} \tag{6}$$

where $r_s^{\min}$ is the minimum canopy resistance ($s\,m^{-1}$) and LAI is the leaf area index ($m^2\,m^{-2}$). F_1, F_2, F_3 and F_4 are weighting functions (–) representing the effects of solar radiation, humidity, air temperature and soil moisture on plant stress. Following Chen and Dudhia (2001), the weighting functions can be expressed as:

$$\begin{aligned} F_1 &= \frac{r_s^{\min}/r_s^{\max} + f}{1+f} \text{ with } f = 0.55\frac{R_g}{R_{gl}}\left(\frac{2}{LAI}\right) \\ F_2 &= \frac{1}{1 + h_s \times (q^* - q)} \\ F_3 &= 1 - 0.0016\left(T_{ref} - T_a\right)^2 \\ F_4 &= \sum_{i=1}^{N_{root}} \frac{\left(\theta_i - \theta_{wilt}\right) d_i}{\left(\theta_{ref} - \theta_{wilt}\right) d_t} \end{aligned} \tag{7}$$

where $r_s^{\max}$ is the maximum or cuticular canopy resistance ($s\,m^{-1}$), R_{gl} is the minimum solar radiation necessary for transpiration ($W\,m^{-2}$), R_g is the incident solar radiation ($W\,m^{-2}$), h_s is a parameter associated with the water vapour deficit (–), $q^* - q$ represents the water vapour deficit ($kg\,kg^{-1}$), T_{ref} is the optimal temperature for photosynthesis (K), T_a is the air temperature (K), d_i is the thickness of the ith soil layer (m), d_t is the total thickness of the soil layer (m) and N_{root} is the number of soil layers in the rooting zone.

In this study, the depth of the soil moisture sensor(s) is considered to be representative of the soil layer(s). Such an assumption is unlikely to be valid for the cases of vegetation with deep root systems, since the change in surface soil moisture at the half-hourly or hourly time step will not be the same for the whole soil column. However, the limited availability of soil moisture data at tower locations reduces the capacity to improve the assumption further, so some compromise is unavoidable. The values of $r_s^{\max}$, R_{gl}, h_s and T_{ref} are acquired based on the vegetation lookup tables used in the Noah land surface model.

Soil moisture content thresholds for field capacity (θ_{ref}) and wilting point (θ_{wilt}) provide characteristics of the soil type. As soil type information is not available for all sites from field investigations and the values in existing global soil databases are not reliable at the point scale, long-term surface layer soil moisture observations from each tower are used to determine the soil moisture thresholds (Calvet et al., 1998; Ladson et al., 2004; Zotarelli et al., 2010). To do this, the field capacity soil moisture threshold is determined as the 99th percentile of the after rain soil moisture records of the tower. As the short period of soil moisture data might cause lower values of the actual θ_{ref} using this technique, estimated θ_{ref} is truncated to the maximum θ_{ref} value suggested by the soil table used in the Noah land surface model. Similarly, the wilting point threshold is determined from the 1st percentile of the soil moisture records and is capped to the minimum value of the Noah soil table. Both vegetation and soil parameter tables of the Noah model can be obtained from http://www.ral.ucar.edu/research/land/technology/lsm.php.

2.2.3. Advection-aridity (AA): a complementary method

The concept of complementary fluxes with advection-aridity was first developed by Bouchet (1963) and further improved by Parlange and Katul (1992). The complementary relationship relies on the feedback between actual and potential evaporation. When there is sufficient water available, evaporation increases and approaches the potential value. In contrast, when water is limited, the energy that would have been used for evaporation is then used in the production of sensible heat flux. As a result, the vapour pressure deficit increases because of the lack of evaporation, thus elevating the potential evaporation (Huntington et al., 2011). As

shown by Brutsaert (2005), the advection-aridity equation for estimation of evaporation (E) is:

$$E = (2\alpha_{PT} - 1)\frac{\Delta}{\Delta+\gamma}Q_{ne} - \frac{\gamma}{\Delta+\gamma}\frac{\rho(q^* - q)}{r_a} \quad (8)$$

where α_{PT} is the Priestley–Taylor coefficient, considered here as 1.26 (Priestley and Taylor, 1972; Eichinger et al., 1996), q is the specific humidity of the atmosphere ($kg\,kg^{-1}$) and q^* is the specific humidity of the saturated air ($kg\,kg^{-1}$) at temperature T_a. Also, $Q_{ne} = Q_n/\lambda$ with Q_n being available energy, defined as $Q_n = R_n - G$. Parameterization of the aerodynamic resistance r_a in this study is similar to that used for the Penman–Monteith model (Brutsaert and Stricker, 1979; Brutsaert, 2005). The main advantage of the advection-aridity complementary approach is that it does not require any information related to soil moisture, canopy resistance or other measures of aridity, as it relies solely on meteorological variables.

2.2.4. Modified Priestley–Taylor (PT-JPL): a radiation based scheme

The Priestley–Taylor model (Priestley and Taylor, 1972) is a simplified form of the Penman–Monteith model, developed for estimating potential evaporation from an extensive wet surface under conditions of minimum advection (Pereira and Villa Nova, 1992; Eichinger et al., 1996; Sumner and Jacobs, 2005). This model is expressed by the following equation:

$$\lambda E = \alpha_{PT}\frac{\Delta}{\Delta+\gamma}(R_n - G) \quad (9)$$

Scaling of the Priestley–Taylor potential evaporation to actual evaporation has been performed by modification or calibration of α_{PT} (Flint and Childs, 1991) as a function of the environmental variables. However, in this study we use the modified form of the Priestley–Taylor model developed by Fisher et al. (2008) (hereafter PT-JPL), in which the α_{PT} is kept constant at 1.26 and the potential evaporation is scaled to actual evaporation based on bio-physiological constraints. In this model, total evaporation is partitioned into canopy transpiration (λE_c), soil evaporation (λE_s) and wet canopy evaporation (λE_{wc}) defined as follows:

$$\begin{aligned}\lambda E_c &= k_c \times \alpha_{PT}\frac{\Delta}{\Delta+\gamma}R_n^c \\ \lambda E_s &= k_s \times \alpha_{PT}\frac{\Delta}{\Delta+\gamma}\left(R_n^s - G\right) \\ \lambda E_{wc} &= k_{wc} \times \alpha_{PT}\frac{\Delta}{\Delta+\gamma}R_n^c\end{aligned} \quad (10)$$

where R_n^c is the net radiation for canopy, $R_n^c = R_n - R_n^s$ and R_n^s is the net radiation for soil given by $R_n^s = R_n \exp(-0.6LAI)$. Total evaporation is then $\lambda E = \lambda E_c + \lambda E_s + \lambda E_{wc}$.

k_c, k_s and k_{wc} are reduction functions for scaling of potential evaporation in each of canopy, soil and wet canopy components to their actual values and are defined as:

$$\begin{aligned}k_c &= (1 - f_{wet})f_g f_T f_M \\ k_s &= f_{wet} + f_{SM}(1 - f_{wet}) \\ k_{wc} &= f_{wet}\end{aligned} \quad (11)$$

where f_g is green canopy fraction, f_{wet} is relative surface wetness and f_T is air temperature constraint, and f_M and f_{SM} are empirical factors used as a proxy for plant and soil water stress, respectively. The reduction functions are defined as:

$$\begin{aligned}f_{wet} &= RH^4 \\ f_g &= f_{APAR}/f_{IPAR} \\ f_T &= \exp\left[-\left(T_a - T_{opt}/T_{opt}\right)^2\right] \\ f_M &= f_{APAR}/f_{APAR_{max}} \\ f_{SM} &= RH^{VPD}\end{aligned} \quad (12)$$

where f_{APAR} and f_{IPAR} are fractions of the photosynthesis active radiation (PAR) that is absorbed ($APAR$) and intercepted ($IPAR$) by green vegetation cover, defined as $f_{APAR} = 1.3632 \times SAVI - 0.048$ and $f_{IPAR} = NDVI - 0.05$. RH represents the relative humidity (fraction), VPD is vapour pressure deficit in kPa and the leaf area index, LAI, is calculated as $LAI = -\ln(1 - f_c)/k_{PAR}$ with $k_{PAR} = 0.5$ and $f_c = f_{IPAR}$. The optimum plant growth temperature (T_{OPT}) is the air temperature at the time of peak canopy activity when the highest f_{APAR} and radiation and minimum VPD occur. Finally, $SAVI$ is the soil adjusted vegetation index, calculated as $SAVI = 0.45 \times NDVI + 0.132$.

While Fisher et al. (2008) estimated evaporation using monthly means of tower based meteorological measurements of R_n, maximum T_a and average vapour pressure (e_a), this study uses half-hourly or hourly values of those variables for flux prediction.

2.2.5. Data requirement of the evaporation models

The four evaporation models of this study differ in their required input data and the types of parameterizations employed. The PM model is the most complex and one of the most data-demanding models as a result of aerodynamic and surface resistances requiring the explicit description of a number of variables and parameters. While there is no necessity for surface resistance parameterizations in the SEBS model, it still requires land surface temperature observations and is sensitive to the temperature gradient near the surface. The AA model demands even less prescribed information, as it does not need soil moisture or land surface temperature. Overall, the PT-JPL model is the least data-demanding model used in this study, requiring only air temperature, humidity, net radiation and ground heat flux (see Table 2).

2.3. Statistical evaluations

The statistical measures used to evaluate model performance include the coefficient of determination (R^2), slope, y-intercept, root-mean-squared difference ($RMSD$), relative error (RE) and the Nash–Sutcliffe efficiency coefficient (NSE). The coefficient of determination describes the degree of co-linearity between simulated and observed values and ranges between 0 and 1, with higher values indicating less error variance. In general, an $R^2 > 0.5$ is considered as acceptable performance (Moriasi et al., 2007). RE is defined as the $RMSD$ normalized by the mean values of observed data, with $RE = RMSD/mean(\lambda E_{obs})$. The Nash–Sutcliffe efficiency represents a normalized statistic that determines the relative magnitude of the residual variance (noise) compared to the measured data variance (Nash and Sutcliffe, 1970) and is computed as:

$$NSE = 1 - \left[\frac{\sum_n^{i=1}\left(\lambda E_i^{obs} - \lambda E_i^{sim}\right)^2}{\sum_n^{i=1}\left(\lambda E_i^{obs} - \lambda E_{mean}\right)^2}\right] \quad (13)$$

where λE_i^{obs} is the ith observed λE, λE_i^{sim} is the ith simulated λE, λE_{mean} is the mean of the observed λE and n is the total number of observations. NSE indicates how well the scatterplot of observed versus simulated data fits the 1:1 line. NSE values range between $-\infty$ and 1.0, with a $NSE = 1$ being the optimal value (Moriasi et al., 2007). In addition to the use of single statistics for evaluation of

Table 2
List of required data and parameters for evaporation models as used within this study.

Variable/Parameter	SEBS	AA	PM	PT-JPL
Land surface temperature	×			
Air temperature	×	×	×	×
Wind speed	×	×	×	
Humidity	×	×	×	×
Roughness parameters	×	×	×	
Soil moisture			×	
Net radiation	×	×	×	×
Ground heat flux	×	×	×	×
Soil/Vegetation parameters			×	
Vegetation index (e.g. *NDVI*)	×	×	×	×

each tower, average values of *NSE*, R^2 or *RE* values for all towers of a biome (or of all 20 towers) are used as NSE_{avg}, R^2_{avg} and RE_{avg} for the cases in which an overall assessment of the models is required.

A general assumption in interpretation of the slope, *y*-intercept, R^2, *RE* and *NSE* is that all of the errors are contained within the simulated values, such that the observed values are error free. This assumption is rarely the case, as λE observations are uncertain due to a number of factors including representativeness of the source area, instrument sampling errors, land surface heterogeneity and random observation error. Recent work examining the impacts of forcing data error on model simulations of heat fluxes highlights the importance of characterizing the inherent observation error (Ershadi et al., 2013b).

2.4. Energy budget closure at flux tower sites

In evaluation of the heat flux models at short time intervals (e.g. hourly), the so-called non-closure issue has been observed by many researchers (e.g. Twine et al., 2000; Massman and Lee, 2002; Barr et al., 2006; Haverd et al., 2007; Franssen et al., 2010). The lack of closure in energy balance at eddy covariance towers remains largely unexplained. Likewise, the best way to handle it in terms of data correction remains an open question (Foken et al., 2012). Many studies have shown that this non-closure problem is not due to the uncertainty and errors in observations alone. For example, Mauder and Foken (2006) showed that even at a well maintained site, careful application of all corrections to the raw high-frequency data can slightly reduce the residuals, but cannot completely remove them. One reason for the lack of closure in eddy covariance sites is attributed to unaccounted for advection fluxes. In addition, large eddies (with low frequency) associated with stationary secondary circulations (Foken, 2008; Mahrt, 2010) that generate over tall canopies and heterogeneous landscape are not usually measured at eddy covariance towers due to instrument limitations (Mauder et al., 2008; Foken et al., 2011, 2012). Kracher et al. (2009) attributed the lack of closure in energy balance to the ground heat flux or storage of the energy in the plant canopy. However, correction for this might result in a large ground heat flux or storage term that cannot be explained by the storage capacity of the soil or canopy (Foken et al., 2011).

One relatively simple way to account for the residual errors in turbulent heat flux measurements is to distribute them according to the Bowen ratio (i.e. $\beta = H/\lambda E$). This method is referred to as the "Bowen ratio" closure correction technique (Twine et al., 2000). Alternatively, the lack of closure can also be corrected by calculating the latent heat flux as a residual term in the energy balance equation (i.e. $\lambda E_{ER} = R_n - G - H$) using the observed fluxes. This method is referred to as the "energy residual" closure correction technique. Either way, both techniques have a major and potentially adverse effect on the actual energy and water balance within the system being examined (Foken, 2008).

In this study, both the "Bowen ratio" (BR) and "energy residual" (ER) closure correction techniques were evaluated against modelled evaporation. Following Sumner and Jacobs (2005), the Bowen ratio correction is applied as:

$$\lambda E_{BR} = \frac{R_n - G}{1 + \beta} \tag{14}$$

The corrected latent heat flux values that were less than half or more than double the uncorrected values were considered as missing data (less than 10% amongst all towers). The *NSE* coefficient of the simulated latent heat fluxes calculated against the original, energy residual (ER) corrected and Bowen ratio (BR) corrected data are shown in Fig. 2. A similar figure showing R^2 values is added to the supplementary materials (Fig. S6).

Fig. 2 illustrates that for the majority of model types and land surface conditions, the simulated latent heat fluxes show improved agreement when employing the energy residual corrected latent heat fluxes. This agreement is perhaps because the ER corrected latent heat fluxes are based on the observed sensible heat fluxes rather than the observed latent heat fluxes. In other words, there may be a potential error source in the observed latent heat fluxes that influences their agreement with the modelled values.

Foken et al. (2011) attributed the reasons for lack of performance in Bowen ratio corrected latent heat fluxes to two concepts. The first is the lack of scalar similarity in sensible and latent heat fluxes (Finnigan et al., 2003; Ruppert et al., 2006; Mauder et al., 2008), which requires that these scalar quantities are transported with similar proportion in eddies of different size and shape. In particular, there are differences in turbulent exchanges for temperature and water vapour in tall and dense canopies, which result from dissimilarity of the sources for sensible and latent heat fluxes. This means that while the canopy top is the main source for heating of air during the day, the source of water vapour is predominantly from within the canopy (Katul et al., 1995, 1999; Simpson et al., 1998; Ruppert et al., 2006). Subsequently, if there is no similarity between sensible and latent heat fluxes, the correction based on the Bowen ratio fails. A possible reason for the improved agreement in the BR corrected latent heat fluxes with the PM based simulations (see Fig. 2) relative to the other model approaches, might be due to the explicit assumption of the Bowen ratio concept (i.e. similarity between sensible and latent heat fluxes) in the derivation of the PM equation. The second concept stated by Foken et al. (2011), relates to the difference in reliability of the eddy covariance system sensors. Maintaining the calibration of the infrared gas analyser (IRGA) sensor, which monitors the humidity fluctuations, is challenging. The IRGA sensor also has higher sensitivity in capturing the large eddies. In contrast, the sonic anemometer sensor can measure the fluctuation of the sonic temperature with greater reliability. Hence, more errors can be expected in the latent heat flux measurement than those of the sensible heat flux.

Accordingly, the energy residual (ER) corrected latent heat fluxes are used as the basis for evaluation of the evaporation models of this study. It is important to note that the latent heat fluxes

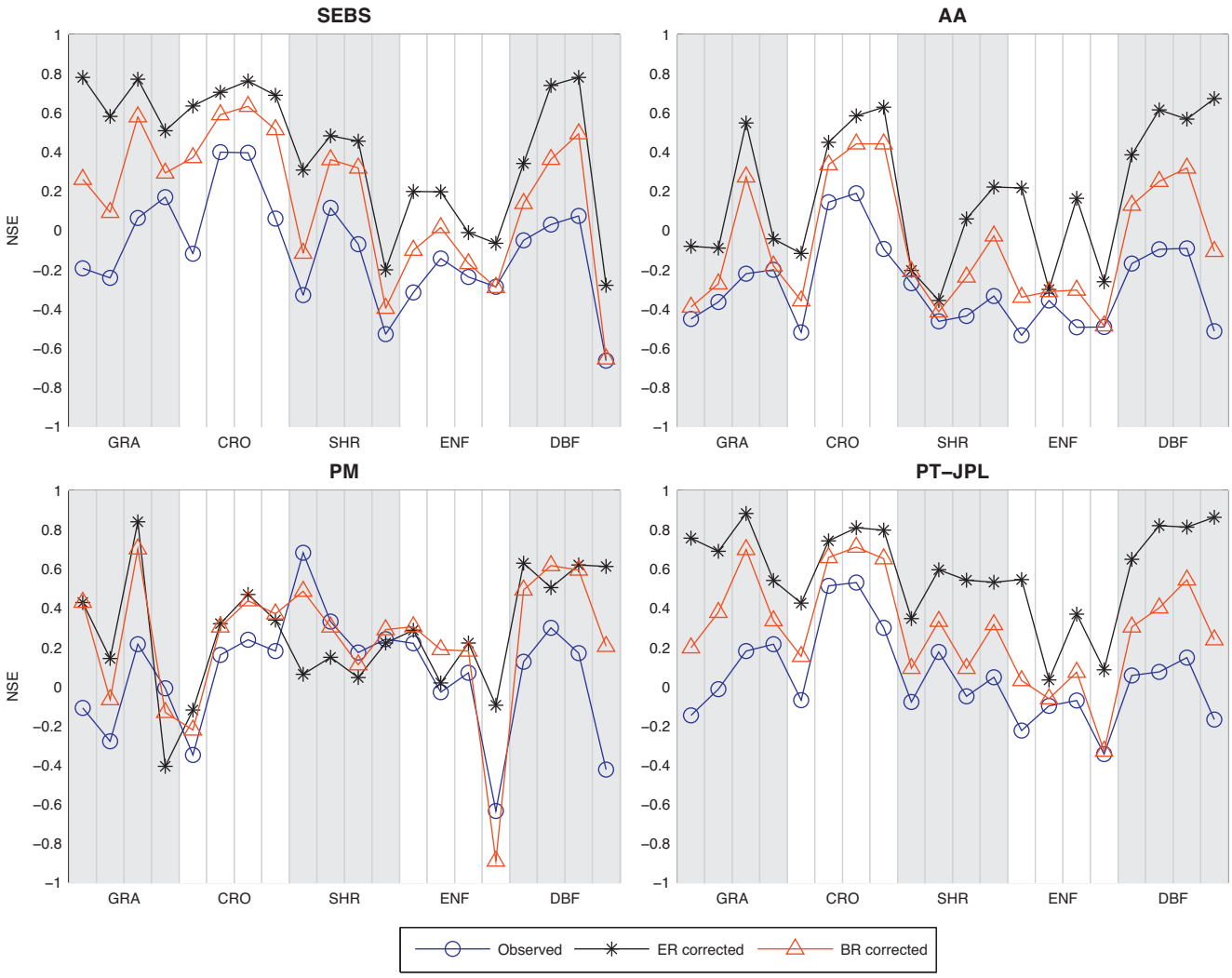

Fig. 2. Comparison of Nash–Sutcliffe efficiency coefficient calculated for simulated latent heat flux versus observed, energy residual (ER) corrected and Bowen ratio (BR) corrected ones. GRA = grassland, CRO = cropland, SHR = shrubland, ENF = evergreen needleleaf forest, DBF = deciduous broadleaf forest.

estimated using the different evaporation models have a direct fractional (for PM, PT-JPL and AA) or residual (for SEBS) link with the observed available energy. Hence, the modelled latent heat fluxes are not completely independent from the Bowen ratio and/or energy residual closure corrected latent heat fluxes. Such dependencies and correlations might also contribute to the improved agreement that is observed in the energy residual closure correction technique.

3. Results

3.1. Performance of models over the entire data period

In this section, the performance of the evaporation models is studied over the entirety of the available period of data collected for each tower. To do this, the statistical measures introduced in Section 2.3 are calculated for all filtered data (see Section 2.1), with the reference for model simulations being the energy residual (ER) closure corrected latent heat fluxes from measurements at each tower. In addition to the individual model results, an ensemble mean (EM) of the model estimates (with equal weights) is calculated and included in the analyses to develop an overall evaluation of performance. Results are summarized in plots of R^2, *RE* and *NSE* for all towers, as is shown in Fig. 3. Further statistical details on the performance of the models are provided as scatterplots and summary tables in the supplementary material.

In Fig. 3, the biomes are ordered based on the vegetation height, from grasslands on the left to the forest sites on the right. Likewise, within each biome, towers are ordered based on the vegetation height (lowest to highest from left to right) at each site. A similar figure (Fig. S7) is also shown in the supplementary materials with towers arranged from left to right based on total rainfall.

The three selected statistical measures (R^2, *RE*, *NSE*) are relatively consistent in representing the performance of each model over each tower. Generally, PT-JPL and SEBS have higher values of R^2 and *NSE* and lower values of *RE*. AA model showed high values of R^2 (comparable to those of PT-JPL and SEBS) over shrublands and forest biomes, but lower values of *NSE* and *RMSD*, meaning that the AA estimates are biased. Accordingly, the performance of the AA and PM models is lower than both SEBS and PT-JPL. The performance of the ensemble mean is comparable to PT-JPL and SEBS over grasslands, croplands and deciduous broadleaf forest, but is higher than any other model across shrublands and evergreen needleleaf forest sites (except for E4). If the mean values of *NSE* and *RMSD* (i.e. the mean of the values shown in Fig. 3 for all towers; represented as NSE_{avg} and $RMSD_{avg}$) are considered as measures for the overall performance of the models, the ensemble mean (EM) presents the best overall performance with $NSE_{avg} = 0.61$

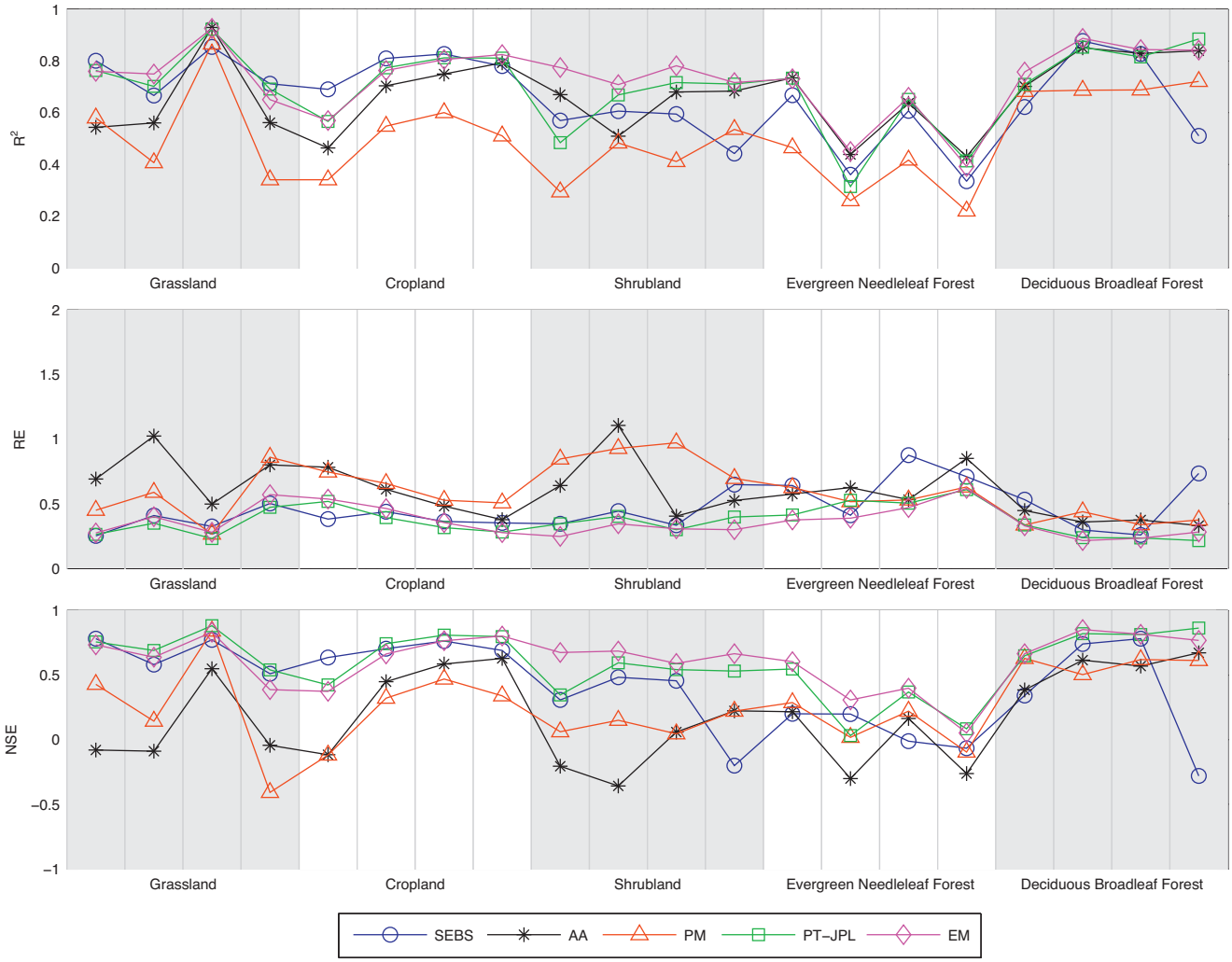

Fig. 3. Comparison of the efficiency of the evaporation models. R^2 is the coefficient of determination, *RE* is relative error (lower is better) and *NSE* is the Nash–Sutcliffe efficiency coefficient (higher is better). Towers in each biome type are arranged from left to right (e.g. G1–G4 for Grassland). EM is for ensemble mean of the models.

and $RMSD_{avg} = 64\,W\,m^{-2}$. Amongst the individual models, PT-JPL model has a good overall performance, with $NSE_{avg} = 0.59$ and $RMSD_{avg} = 66\,W\,m^{-2}$. The second good model is the SEBS with $NSE_{avg} = 0.42$ and $RMSD_{avg} = 84\,W\,m^{-2}$. Amongst the models, the performance of the PM model is ranked third with $NSE_{avg} = 0.26$ and $RMSD_{avg} = 105\,W\,m^{-2}$, while the AA model presents a $NSE_{avg} = 0.18$ and $RMSD_{avg} = 105\,W\,m^{-2}$.

As expected, a model performance varies over the different biomes. In particular, almost all models have lower performance over evergreen needleleaf forest sites, but higher performance over deciduous broadleaf forest sites and cropland sites. Specifically, the SEBS model has good performance for grasslands and croplands with relatively high R^2 (>0.67), moderate relative error ($\leq$0.5), relatively high *NSE* ($\geq$0.5) and slope values close to 1. However, for shrubland and forest sites with taller (>3 m) and heterogeneous canopies, the performance of the SEBS model decreases. As is explained in Section 4.1, the reduced performance of the SEBS model may relate to the presence of the roughness sub-layer of those canopies. The PT-JPL model has R^2 values similar to the SEBS model in grassland and cropland sites, but its slopes are marginally lower (see scatterplots in the supplementary materials), suggesting an underestimation of evaporation. Over tall canopies (>3 m), the PT-JPL model has better performance than the SEBS and other models in terms of *NSE*, slope, *y*-intercept and RMSD. The PM model underestimates evaporation in the majority of towers across each biome type, with low values of slope (e.g. less than 0.75). The model also displays low values of R^2 (e.g. less than 0.5) for some towers in grassland, shrubland and evergreen needleleaf forest biomes. In contrast to the PM model, the AA model shows strong overestimation of evaporation: in particular over grassland and deciduous broadleaf forest sites (slope $\geq$ 1.10). A more comprehensive summary of the performance of the models in each biome type is provided in Table 3.

3.2. Performance of models at monthly timescales

Given the temporal changes in water and energy availability that occur throughout the year, it is of interest to examine the impact of such variations on these different evaporation models. To study possible seasonal influences on the performance of the models (and the ensemble mean), we examined the temporal changes in monthly *NSE* for half-hourly and hourly *E*. For each tower, we first calculated the *NSE* for all half-hourly or hourly data in each month of the multi-year tower records. Then, a single average of those per-month *NSE* values was calculated for each model across each tower, with the results plotted in Fig. 4. A similar figure showing monthly-based R^2 values is also presented in the supplementary materials. To support identifying the temporal trend of *E* at each site, the monthly average of observed *E* for each tower is calculated as μ_E, which is used to calculate the normalized fraction of

Table 3
A summary of the performance of the evaporation models. Biome types are defined as: GRA = grassland, CRO = cropland, SHR = Shrubland, ENF = evergreen needleleaf forest, DBF = deciduous broadleaf forest. The numbers in the parenthesis in each grid are biome averaged R^2_{avg}, RE_{avg} and NSE_{avg} (from left to right). The numbers underneath the biome abbreviations in the first column denote the ranked order of models (SEBS, AA, PM, PT-JPL from left to right) based on their statistical performance (see supplementary materials) over that particular land cover type.

	SEBS	AA	PM	PT-JPL
GRA 4,1,3,2	(0.76; 0.37; 0.66) -Good performance with NSE_{avg} = 0.66 and slope close to 1 - $RMSD \leq 59\,W\,m^{-2}$ and $NSE \geq 0.51$	(0.71; 0.73; 0.21) - Overestimation with slope ≥ 1.1 - Highest *RMSD* values	(0.55; 0.54; 0.25) - Underestimation in all sites except in G3	(0.77; 0.33; 0.72) - Best performance with NSE_{avg} = 0.77 and slope close to 1 - Underestimation at G1 and G2, with slope ≤ 0.83 - Lowest values of *RMSD* (44–55 $W\,m^{-2}$)
CRO 1,4,2,3	(0.78; 0.38; 0.7) - Good performance with tower based $R^2 \geq 0.69$ and $RMSD \leq 68\,W\,m^{-2}$, slope ≥ 0.90 and *y*-intercept ≤ 51 $W\,m^{-2}$	(0.68; 0.56; 0.39) - Overestimation at C1 and C2 with *y*-intercept ≥ 40 - Higher *y*-intercept in C2 (rainfed crop) than C3 (irrigated crop)	(0.5; 0.61; 0.25) - Lower R^2 than other models - Underestimation in C1 and C4 - More scatterness for $\lambda E < 300\,W\,m^{-2}$	(0.74; 0.38; 0.69) - Except in C1, its performance is comparable with the SEBS model
SHR 4,1,3,2	(0.55; 0.44; 0.26) - Good performance for S1, S2 and S4 compared to other models - Underestimation in S3 with slope = 0.8	(0.64; 0.67; −0.07) - Overestimation in S1, S2 and S3 with slope > 1.3	(0.43; 0.86; 0.12) - Underestimation in all sites with slope ≤ 0.3	(0.65; 0.36; 0.5) - Best performance compared to other models - Underestimation in S1 with slope = 0.7
ENF 4,3,1,2	(0.49; 0.66; 0.08) - Overestimation in E1 and E3 with slope = 1.2 - Underestimation in E2 and E4 with slope < 0.6	(0.56; 0.64; −0.05) - Overestimation in E1 and E3 with slope ≥ 1.2 - Overestimation in E2 and E4 with *y*-intercept ≥ 54 $W\,m^{-2}$	(0.34; 0.57; 0.11) - Underestimation in all sites with slope ≤ 0.7	(0.53; 0.51; 0.26) - Good performance in E1 and E3 ($R^2 \geq 0.65$, slope ≅ 1, $RMSD \leq 79\,W\,m^{-2}$) - Underestimation in E2 and E4 with slope ≤ 0.8
DBF 4,3,2,1	(0.71; 0.45; 0.4) - Overestimation in all towers except in D3	(0.81; 0.38; 0.56) - Overestimation with slope ≥ 1.1 - Negative *y*-intercept at D2, D3 and D4	(0.7; 0.37; 0.59) - Underestimation except at D4 - R^2 > 0.68 and *NSE* ≥ 0.5 in all sites	(0.82; 0.25; 0.79) - Best performance with highest *NSE* compared to other models

monthly evaporation (f_E) via equation (15). Time series of f_E are shown in thick grey lines in each panel of Fig. 4.

$$f_E = \frac{\mu_E - \min(\mu_E)}{\max(\mu_E) - \min(\mu_E)} \quad (15)$$

Although the lack of data for some towers will influence the statistical significance of the calculated per-month average values (e.g. there are four towers with less than 2 years of data records), the results are expected to reflect the dominant trends in model performance, since most biomes contain a sufficiently long record.

To evaluate the performance of the models in different seasons, we use the term "seasonality" i.e. a model with high seasonality is a model that only performs well for a few months of the year. Fig. 4 shows that each model has a different behaviour in seasonality at different towers and even at towers that belong to the same biome type. For example, the SEBS model shows better performance in summer months at E3 (DE-Tha), but the opposite (i.e. lower performance in summer) at E4 (US-Wrc). As another example, SEBS shows no seasonality in G1 (PT-Mi2) tower, but some seasonality in G2 (US-Aud) and G3 (US-Goo).

Not discounting the cases mentioned above, some general trends can be observed in the seasonality of the models in Fig. 4. For example, all models (and the ensemble mean) indicate a degree of seasonality in the cropland and deciduous broadleaf forest sites. However, the number of months with higher *NSE* values is lower for PM and the AA models. Moreover, these two models show stronger seasonality than do the SEBS and PT-JPL models. One other important observation is the poor performance of PM, AA and SEBS models over the shrubland sites, showing a number of near-zero or negative values of monthly-based *NSE* during the year. Similar to the observations made for Fig. 3, monthly-based *NSE* values of the ensemble mean are higher than the models in majority of the cases, but they have seasonality trends (mostly similar to PT-JPL seasonality trends).

4. Discussion

The results presented in the sections above are of interest in studying the performance of the evaporation models across different biome types. However, comparison of the results against findings from relevant previous studies can be useful in understanding and diagnosing the main causes for the lack of performance for some models relative to others.

4.1. SEBS model performance

The SEBS model performed well in grassland and cropland sites having short canopies (e.g. less than 3 m) and displayed limited seasonality in its performance over the majority of the examined towers. However, SEBS also showed reduced performance over (tall) forest and (heterogeneous) shrubland landscapes. This limitation of SEBS can be attributed to an uncertainty that exists in the structure of the SEBS model: the form of the MOST equations used in SEBS does not have correction terms to adjust for the so-called roughness sub-layer effects (Harman and Finnigan, 2007; Harman, 2012). This limitation was addressed in a recent contribution by Weligepolage et al. (2012) for a forest site.

Other reasons for the reduced performance of the SEBS model in certain instances might relate to errors in the input data and model parameterizations. For example, SEBS showed reduced performance over shrubland (NSE_{avg} = 0.26) and evergreen needleleaf forest sites (NSE_{avg} = 0.08), where the heterogeneity in the landscape is likely to be strong and the representative source area for various input variables or parameters might be different. In particular, SEBS is sensitive to the terms that control the transfer of heat from the land surface to the atmosphere, including the temperature difference between the land surface and the atmosphere and the parameterization of the aerodynamic resistance. Therefore, any errors and uncertainties in the observations of the land

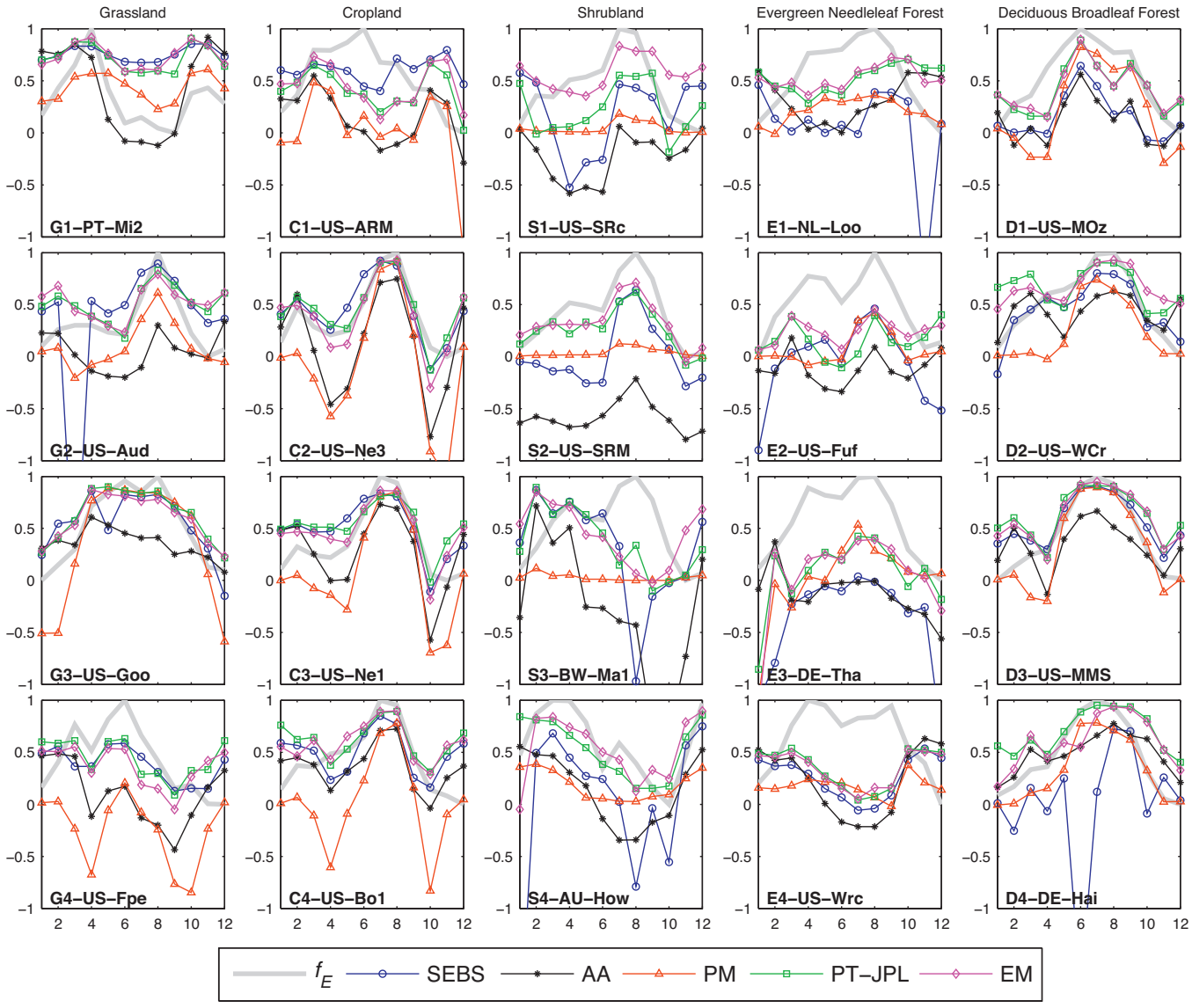

Fig. 4. Mean per-month value of the Nash–Sutcliff efficiency calculated for each of the four studied models at each of the 20 tower locations. The *x*-axis represents month of the year, while each point on the graph represents the temporally averaged per-month *NSE* calculated for all available tower record years (see Table 1 for details on individual tower data length). Note that the per-month *NSE* values are for half-hourly or hourly scale *E* data, not in monthly scale. f_E is normalized fraction of monthly observed *E*. EM is for ensemble mean of the models.

surface temperature, air temperature, wind speed and roughness parameters will directly influence the performance of the SEBS model. Due to the complexity of the heat transfer and energy balance mechanisms and deficiencies in the spatially representative in-situ observations, it is not clear which variable or parameter has a greater role in the final sensible or latent heat product. Consequently, there is no agreement in previous research regarding the main cause of uncertainties in the SEBS model performance. These uncertainties have been attributed to the roughness parameters (Timmermans et al., 2013), land surface temperature errors (van der Kwast et al., 2009) or total errors in the temperature gradient and wet limit criteria (Gibson et al., 2011).

In a recent contribution, Ershadi et al. (2013b) used a Bayesian inference technique to quantitatively estimate the errors and uncertainties of input data in estimation of the sensible heat flux over soybean and corn towers in the SMEX02 (Soil Moisture Experiment 2002) study area. They showed that amongst air temperature, wind speed and land surface temperature, the latter had the strongest effect on the mismatch between observed and estimated sensible heat flux, with Bayesian inferred values of the land surface temperature differing by up to ±5 °C from the in-situ observed data. They attributed such difference to the divergence between the footprint of the in-situ land surface temperature sensor and the footprint of the eddy covariance tower. As the heterogeneity of the land surface in the majority of the towers in this study is much stronger than those of the SMEX02 study area, it might be relevant to assume larger differences in the source area (footprint) of meteorological variables than those of the flux variables, which contribute to explaining a large degree of errors observed in the SEBS results.

4.2. AA model performance

The AA model showed relatively high values of R^2_{avg} (comparable with those of PT-JPL and SEBS), but its overall lower performance (NSE_{avg} = 0.18 and $RMSD_{avg}$ = 105 W m^{-2}) was associated with relatively large overestimation of evaporation (e.g. slope ≥ 1.05) across all biomes. Comparison of the results of this study with previous

research is not completely feasible, due to different forms of wind functions being used for aerodynamic resistance (Crago et al., 2005) and in some cases, model parameters being calibrated (Liu et al., 2012). However, the seasonality (underestimation in winter or dry condition) and significant biases, in particular over grassland and deciduous broadleaf forest sites, have been observed and documented in previous studies (Ali and Mawdsley, 1987; Crago and Brutsaert, 1992; Qualls and Gultekin, 1997; Hobbins et al., 2001; Crago and Crowley, 2005). For example, Han et al. (2011) observed significant bias in evaporation estimations of the advection-aridity model over different grassland and cropland sites of China. Also, Huntington et al. (2011) evaluated a modified advection-aridity model over arid shrublands in eastern Nevada and found monthly evaporation overestimated, but the annual averages (for 2 years) were within the uncertainty of the measurement accuracy (~10%).

A possible explanation for the errors found in the current evaluation of the AA model might be associated with the assumption of a constant α_{PT} for all towers. While the original AA model does not require calibration of its α_{PT} parameter, some studies have shown that the Priestley–Taylor coefficient (α_{PT}) varies for different regions and with vegetation type. For example, Pauwels and Samson (2006) observed an annual cycle in the calculated values of α_{PT} with mean annual average value of 1.21 ± 0.79 over grass, which they found is related to the annual cycle of the humidity of the soil. In addition, Yang et al. (2013) found that α_{PT} in the AA model has significant seasonality in the Asian monsoon region, with larger α_{PT} value in winter than in summer.

The poor performance of the AA model over shrubland and forest sites ($NSE_{avg} = 0.15$ and $RMSD_{avg} = 108\ W\ m^{-2}$) might be associated with the assumption of a neutral atmosphere that is intrinsic in the formulation of this model (Brutsaert, 1982). This assumption is invalid over tall and heterogeneous land surfaces where the instability in the turbulence is significant and the roughness sub-layer might influence eddy covariance measurements. In addition, as noted for the SEBS model, errors and uncertainties in input data and roughness parameterization and mismatch between the sources areas for input and response variables, all contribute to the low performance of the AA model.

4.3. PM model performance

Although widely used across a range of land cover and climate conditions, the results of this study identified some limitations in the application of the form of the Penman–Monteith approach used in this study ($NSE_{avg} = 0.26$ and $RMSD_{avg} = 105\ W\ m^{-2}$). In many instances, there was a significant underestimation of evaporation (slope ≤ 0.9) and considerable seasonality over a number of towers: in particular, those situated in croplands or in deciduous forests. The seasonality results indicated that in the colder months the performance of the model is limited, with large errors resulting in an underestimation of evaporation.

Similar challenges in the performance of the PM model have been identified in a number of previous studies, where errors were attributed to the land surface conditions and uncertainties in input data. For example, Burba and Verma (2005) identified that the difference in PM estimations of evaporation in native tallgrass prairie and cultivated wheat, is strongly related to the effects of soil moisture stress and variations in green foliage area, with meteorological variables having a smaller impact. Conversely, Ferguson et al. (2010) found that the choice of vegetation parameterization, followed by surface temperature, has the greatest impact on PM derived evaporation.

Given the multi-model scheme of this study, comparison with the PT-JPL model would provide a practical means to identify some of the limitations of the PM model. In particular, it might be expected that if high-quality input data were used, this model should outperform the PT-JPL model given the theoretical advances of the PM approach over the PT-JPL model (see Sections 2.2.2 and 2.2.4). However, an evaluation of a single-source PM model (similar to that of the current study), the two-layer Shuttleworth and Wallace (1985) and the three-source Mu et al. (2011) model with a range of r_a and r_s parameterization techniques (for the same towers of this study) (Ershadi et al., 2013a) has shown that resistance parameterization, in particular the surface resistance, has an important role in PM type models: indeed, more important than the actual structure of the model. As such, better performance of the PT-JPL model (compared to the PM model) is related to an effective use of biological and environmental constraints in reducing the potential Priestley–Taylor E to its actual values, not necessarily to just the E partitioning structure of the PT-JPL method.

In summary, the possible sources of uncertainty in the PM model might be related to: (a) uncertainties inherent in the structure of the Jarvis scheme for surface resistance estimation (Alves et al., 1998; Kumar et al., 2011); (b) errors associated with the soil moisture data that influence the estimation of surface resistance; and (c) uncertainties in the estimation of aerodynamic resistance (e.g. assumption of neutral stability) (Brutsaert, 1982; Mahrt and Ek, 1984). As the PM model shows reduced performance with the high-quality tower scale dataset of this study, some caution is prudent for application of this model at increased spatial scales in which data might be expected to contain larger uncertainties: at least with the model structure and parameterizations used within the current study.

4.4. PT-JPL model performance

Overall and amongst individual models, the PT-JPL model displayed the most consistent performance ($NSE_{avg} = 0.59$ and $RMSD_{avg} = 66\ W\ m^{-2}$) suggesting that it can be considered as a reliable model for evaporation estimation over a range of land surface conditions. However, in the majority of cases (e.g. G1, C3, S1, E3, D3) the performance of PT-JPL and SEBS were close. The PT-JPL approach showed limited seasonality in model performance (see Section 3.2) relative to other models and provided the highest statistical measures of agreement to the observations. Similar performance has been reported by Fisher et al. (2008), with an average R^2 of 0.9 and 7% bias for monthly data for a 3-year period over 16 FLUXNET sites (some of which are included in the current study). More recently, Vinukollu et al. (2011b) identified superior performance of the PT-JPL model in 12 eddy covariance towers, located in grasslands, croplands and woody savannahs, for a 3-year period using monthly averages of hourly data. However, they found significant bias in summer months, which corresponds to the growing season.

Results from the current study show that the PT-JPL is relatively insensitive to the vegetation height and consequently to the roughness sub-layer effects, in contrast to the SEBS model – the next best performing model. The PT-JPL approach does not require the specification of aerodynamic and surface resistances. As such, uncertainties in the estimation of the roughness length parameters have no influence on evaporation estimates in the PT-JPL model. The PT-JPL model requires a minimum of input variables, including *NDVI*, air temperature, available energy and humidity (see Table 2). Therefore, propagation of uncertainties from other variables such as land surface temperature, wind speed and soil moisture provide no adverse influences on this model. Moreover, the PT-JPL model relies on plant functions and bio-physiological parameterization of the land surface that provide a simple yet seemingly robust representation of the interactions between vegetation and the atmosphere. The net radiation and air temperature

are the main driving forces for the PT-JPL model and they generally have lower uncertainty in observations (hence resulting in better model performance) (Table 3).

The PT-JPL model did exhibit reduced performance over the evergreen needleleaf forest towers, which might be attributed to the limitation of *NDVI* in capturing the vegetation dynamics of this biome (Xiao et al., 2004). Consequently, such uncertainties in *NDVI* estimation are translated to errors in the estimation of the constraint function parameters (f_{wet}, f_g, f_T, f_M, f_{SM}) of the PT-JPL model over the evergreen needleleaf forests. Although the PT-JPL model performed well compared to other models of this study, the sensitivity of this model to its constraint function parameters and to the α_{PT} parameter for different land surface conditions are issues worth further investigation. One recent contribution (García et al., 2013) examined a sensitivity analysis of the PT-JPL model at the daily scale over an open woody savannah (Sahel) and Mediterranean grassland (Spain) site. The authors found that f_{SM} and f_T are the most sensitive parameters, contributing to the uncertainty of the estimated evaporation by 22% and 18% respectively. Such figures are useful in determining the main causes of uncertainty in evaporation estimation by the PT-JPL model, in particular in the global applications of this model.

4.5. Performance of the ensemble mean method

The ensemble mean of the models produced the best overall estimates of E across the towers, with $NSE_{avg} = 0.61$ and $RMSD_{avg} = 64\ W\ m^{-2}$. The method also showed limited seasonality trends (similar to PT-JPL) in monthly-based E prediction. The overall *NSE* values of the ensemble mean method (Fig. 3) were comparable to those of the PT-JPL method over individual towers for grasslands, croplands and deciduous broadleaf forest biomes in majority of the cases. However, over shrublands and evergreen needleleaf forest sites, where all the models performed relatively poorly, the ensemble mean method produced higher *NSE* values (except for E3 and E4). Such results may be helpful for large scale applications, where selecting a single candidate E model is challenging (Jiménez et al., 2011; Vinukollu et al., 2011a; Ferguson et al., 2012; Mueller et al., 2013).

Multimodel ensemble approaches are used in hydrological assessment of climate change scenarios (Christensen and Lettenmaier, 2006; Graham et al., 2007; Sheffield and Wood, 2008), climate change projections (Tebaldi and Knutti, 2007), groundwater assessment (Neuman, 2003), hydrological modelling for streamflow prediction (Wood and Rodríguez-Iturbe, 1975; Duan et al., 2007) and remote sensing soil moisture estimation (Guo et al., 2007). However, applications of multimodel ensemble approaches for E estimations are limited to relatively few cases exploring the spatial variability of E at global scales (Vinukollu et al., 2011a; Mueller et al., 2013). Further research is needed to develop and evaluate an effective multimodel ensemble approach for large scale E estimation, perhaps by using probabilistic (e.g. Bayesian) approaches for weighting the models based on their skills for various biomes and climates.

5. Conclusion

In this study, four evaporation models were evaluated over a multi-tower database at hourly or half-hourly temporal resolutions. Models differed in their assumptions, data requirements and parameterization, ranging from comprehensive and complex approaches such as the Penman–Monteith and energy balance schemes, to more simple and semi-empirical approaches, such as the Priestley–Taylor and advection-aridity techniques. Results showed that an ensemble average of the models produced the best performance in evaporation prediction. Amongst the individual models, the PT-JPL model, followed closely by the SEBS model, provided improved performance relative to the PM, as parameterized in Section 2.2.2, and the AA models.

Results of this model intercomparison offer guidance on areas of research that are needed to address some outstanding issues in the application of these models. One such area is in the quantification of the total (integrated) uncertainties for model simulations. Such "integrated" uncertainty would comprise the uncertainties in model structure (e.g. formulation, partitioning), parameterization (e.g. roughness, resistances), input data (e.g. meteorological data) and response variables (e.g. latent heat flux). Differences between the spatial resolution of point scale input data and model parameters derived from satellite data, as well as footprint difference between input data (e.g. land surface temperature) and observed fluxes, also contribute to these elements of uncertainty (McCabe and Wood, 2006; Ershadi et al., 2013c). Discriminating these various sources of error within model simulations would allow for the diagnosis and identification of the main sources of errors in evaporation estimation. A Bayesian type approach might be useful in handling such uncertainties, while conserving the model context (Kavetski et al., 2006; Samanta et al., 2007; Mackay et al., 2012; Ershadi et al., 2013b). In such a Bayesian uncertainty framework, the non-closure of energy sources can be included as an error source in the response variables.

A further issue in the evaluation of E models is the role of temporal resolution. In the current study, the focus was on hourly and half-hourly resolutions, principally because E models are strictly valid only in steady state conditions (i.e. captured at periods of $\leq$1 h) (Brutsaert, 1982; Katerji et al., 2010). At coarser temporal resolutions (e.g. daily, monthly), the modelling performance might be expected to increase due to an elimination of closure issues (Finnigan et al., 2003) or the noise-reduction mechanism of temporal averaging on input data and measured E. An assessment of temporal aggregation effects on both input data and the flux products is recommended, as many studies use aggregation to daily and monthly scales, without first assessing the impact of uncertainties on model results (Crago and Brutsaert, 1992; Xu and Chen, 2005; Schneider et al., 2007; Vinukollu et al., 2011b).

The sensitivity of some of the models examined here to variations in the underlying land surface conditions implies a need for caution in efforts towards routine global application. Perhaps the key message of this analysis is that one single model is not able to outperform all others when considered across a range of landscapes. That is, there might not be one scheme appropriate for all land cover types. Yet, this remains the predominant approach when developing global flux data sets: a single solution, single model product. For global products to provide useful insight across the diverse terrestrial landscapes encountered in global application, an alternative approach is required. The improved results obtained from the ensemble mean method of this study suggests constructing an ensemble evaporation product, whereby individual products are weighted according to their performance over particular land cover types, might be a reliable candidate approach. To do this requires an expansion on the type of evaluation effort undertaken here, extrapolating across more towers, different land cover types (bare soil, snow, water bodies) and over longer time periods. With the expanding array of available flux towers, computational resources and data sets with which to drive these different modelling schemes, such an approach is certainly achievable for future product development. Recent activities within the GEWEX LandFlux initiative (Mueller et al., 2013) and also within the WACMOS ET project (http://wacmoset.estellus.eu), may provide a potential

framework for implementation of such multi-model ensemble *E* products.

Acknowledgements

Funding for this research was provided via an Australian Research Council (ARC) Linkage (LP0989441) and Discovery (DP120104718) project, together with a top-up scholarship to support Ali Ershadi from the National Centre for Groundwater Research and Training (NCGRT) in Australia. We thank the FLUXNET site investigators for allowing us to use their meteorological data. This work used eddy covariance data acquired by the FLUXNET community and in particular by the AmeriFlux (U.S. Department of Energy, Biological and Environmental Research, Terrestrial Carbon Program: DE-FG02-04ER63917 and DE-FG02-04ER63911) and OzFlux. We acknowledge the financial support to the eddy covariance data harmonization provided by CarboEuropeIP, FAO-GTOS-TCO,iLEAPS, Max Planck Institute for Biogeochemistry, National Science Foundation, University of Tuscia, Université Laval and Environment Canada and US Department of Energy and the database development and technical support from Berkeley Water Center, Lawrence Berkeley National Laboratory, Microsoft Research eScience, Oak Ridge National Laboratory, University of California - Berkeley, University of Virginia. Data supplied by T. Kolb, School of Forestry, Northern Arizona University, for the US-Fuf site was supported by grants from the North American Carbon Program/USDA NRI (2004-35111-15057; 2008-35101-19076), Science Foundation Arizona (CAA 0-203-08) and the Arizona Water Institute. Matlab scripts for automatic downloading of MOD13Q1 data were provided by Dr Tristan Quaife, University College London via the web portal at http://daac.ornl.gov/MODIS/MODIS-menu/modis_webservice.html. We acknowledge the contributions provided via the LandFlux-EVAL initiative and the WACMOS ET project.

Appendix A. Supplementary data

Supplementary material related to this article can be found, in the online version, at http://dx.doi.org/10.1016/j.agrformet.2013.11.008.

References

Agarwal, D.A., Humphrey, M., Beekwilder, N.F., Jackson, K.R., Goode, M.M., van Ingen, C., 2010. A data-centered collaboration portal to support global carbon-flux analysis. Concurrency Computat. Pract. Exp. 22 (17), 2323–2334.

Ali, M.F., Mawdsley, J.A., 1987. Comparison of two recent models for estimating actual evapotranspiration using only regularly recorded data. J. Hydrol. 93 (3–4), 257–276.

Allen, R.G., 2000. Using the FAO-56 dual crop coefficient method over an irrigated region as part of an evapotranspiration intercomparison study. J. Hydrol. 229 (1–2), 27–41.

Allen, R.G., Perista, L.S., Raes, D., Smith, M., 1998. Crop Evapotranspiration – Guidelines for Computing Crop Water Requirements; FAO Irrigation and Drainage Papers – 56. FAO - Food and Agriculture Organization of the United Nations, Rome.

Alves, I., Perrier, A., Pereira, L.S., 1998. Aerodynamic and surface resistances of complete cover crops: how good is the big leaf? Trans. ASAE 41 (2), 345–351.

Baldocchi, D., Falge, E., Gu, L.-H., Olson, R., Hollinger, D., Running, S., Anthoni, P., Bernhofer, Ch., Davis, K., Evans, R., Fuentes, J., Goldstein, A., Katul, G., Law, B., Lee, X.H., Malhi, Y., Meyers, T., Munger, W., Oechel, W., Paw, K.T., Pilegaard, K., Schmid, H.P., Valentini, R., Verma, S., Vesala, T., Wilson, K., Wofsy, S., 2001. FLUXNET: a new tool to study the temporal and spatial variability of ecosystem–scale carbon dioxide water vapor, and energy flux densities. Bull. Am. Meteorol. Soc. 82 (11), 2415–2434.

Barr, A.G., Morgenstern, K., Black, T.A., McCaughey, J.H., Nesic, Z., 2006. Surface energy balance closure by the eddy-covariance method above three boreal forest stands and implications for the measurement of the CO2 flux. Agri. Forest Meteorol. 140 (1–4), 322–337.

Beljaars, A.C.M., Holtslag, A.A.M., 1991. Flux parameterization over land surfaces for atmospheric models. J. Appl. Meteorol. 30 (3), 327–341.

Bormann, H., 2011. Sensitivity analysis of 18 different potential evapotranspiration models to observed climatic change at German climate stations. Clim. Change 104 (3), 729–753.

Bouchet, R.J., 1963. Evapotranspiration réelle, evapotranspiration potentielle, et production agricole. Ann. Agron. 14, 743–824.

Bowen, I.S., 1926. The ratio of heat losses by conduction and by evaporation from any water surface. Phys. Rev. 27 (6), 779–787.

Brutsaert, W., 1982. Evaporation into the Atmosphere: Theory History and Applications. Reidel Publishing, Dordrecht etc, pp. 299.

Brutsaert, W., 1999. Aspects of bulk atmospheric boundary layer similarity under free-convective conditions. Rev. Geophys. 37 (4), 439–451.

Brutsaert, W., 2005. Hydrology: An Introduction. Cambridge University Press, Cambridge, pp. 605.

Brutsaert, W., Stricker, H., 1979. An advection-aridity approach to estimate actual regional evapotranspiration. Water Resour. Res. 15 (2), 443–450.

Burba, G.G., Verma, S.B., 2005. Seasonal and interannual variability in evapotranspiration of native tallgrass prairie and cultivated wheat ecosystems. Agric. Forest Meteorol. 135 (1–4), 190–201.

Calvet, J.C., Noilhan, J., Bessemoulin, P., 1998. Retrieving the root-zone soil moisture from surface soil moisture or temperature estimates: a feasibility study based on field measurements. J. Appl. Meteorol. 37 (4), 371–386.

Cavanaugh, M.L., Kurc, S.A., Scott, R.L., 2011. Evapotranspiration partitioning in semiarid shrubland ecosystems: a two-site evaluation of soil moisture control on transpiration. Ecohydrology 4 (5), 671–681.

Chen, F., Dudhia, J., 2001. Coupling an advanced land surface – hydrology model with the Penn State–NCAR MM5 modeling system. Part I: model implementation and sensitivity. Mon. Weather Rev. 129 (4), 569–585.

Christensen, N., Lettenmaier, D.P., 2006. A multimodel ensemble approach to assessment of climate change impacts on the hydrology and water resources of the Colorado River basin. Hydrol. Earth Syst. Sci. Discuss. 3 (6), 3727–3770.

Cleugh, H.A., Leuning, R., Mu, Q., Running, S.W., 2007. Regional evaporation estimates from flux tower and MODIS satellite data. Remote Sens. Environ. 106 (3), 285–304.

Crago, R., Crowley, R., 2005. Complementary relationships for near-instantaneous evaporation. J. Hydrol. 300 (1–4), 199–211.

Crago, R., Hervol, N., Crowley, R., 2005. A complementary evaporation approach to the scalar roughness length. Water Resour. Res. 41 (6), W06017.

Crago, R.D., Brutsaert, W., 1992. A comparison of several evaporation equations. Water Resour. Res. 28 (3), 951–954.

Curtis, P.S., Hanson, P.J., Bolstad, P., Barford, C., Randolph, J.C., Schmid, H.P., Wilson, K.B., 2002. Biometric and eddy-covariance based estimates of annual carbon storage in five eastern North American deciduous forests. Agric. Forest Meteorol. 113 (1), 3–19.

Delpierre, N., Soudani, K., Francois, C., Köstner, B., Pontailler, J.Y., Nikinmaa, E., Misson, L., Aubinet, M., Bernhofer, C., Granier, A., 2009. Exceptional carbon uptake in European forests during the warm spring of 2007: a data–model analysis. Glob. Change Biol. 15 (6), 1455–1474.

Doorenbos, J., Pruitt, W.O., 1975. Guidelines for Predicting Crop Water Requirements. Irrigation and Drainage Paper.

Dragoni, D., Schmid, H.P., Wayson, C.A., Potter, H., Grimmond, C.S.B., Randolph, J.C., 2011. Evidence of increased net ecosystem productivity associated with a longer vegetated season in a deciduous forest in south-central Indiana, USA. Glob. Change Biol. 17 (2), 886–897.

Duan, Q., Ajami, N.K., Gao, X., Sorooshian, S., 2007. Multi-model ensemble hydrologic prediction using Bayesian model averaging. Adv. Water Resour. 30 (5), 1371–1386.

Eichinger, W.E., Parlange, M.B., Stricker, H., 1996. On the concept of equilibrium evaporation and the value of the Priestley-Taylor coefficient. Water Resour. Res. 32 (1), 161–164.

Ershadi, A., McCabe, M.F., Evans, J.P., Chaney, N.W., Wood, E.F., 2013a. Significance of model structure and parameterization on Penman-Monteith type evapotranspiration models. J. Hydrol., in review.

Ershadi, A., McCabe, M.F., Evans, J.P., Mariethoz, G., Kavetski, D., 2013b. A Bayesian analysis of sensible heat flux estimation: quantifying uncertainty in meteorological forcing to improve model prediction. Water Resour. Res. 49 (5), 2343–2358.

Ershadi, A., McCabe, M.F., Evans, J.P., Walker, J.P., 2013c. Effects of spatial aggregation on the multi-scale estimation of evapotranspiration. Remote Sens. Environ. 131, 51–62.

Ferguson, C.R., Sheffield, J., Wood, E.F., Gao, H., 2010. Quantifying uncertainty in a remote sensing-based estimate of evapotranspiration over continental USA. Int. J. Remote Sens. 31 (14), 3821–3865.

Ferguson, C.R., Wood, E.F., Vinukollu, R.K., 2012. A global intercomparison of modeled and observed land–atmosphere coupling*. J. Hydrometeorol. 13 (3), 749–784.

Finnigan, J.J., Clement, R., Malhi, Y., Leuning, R., Cleugh, H.A., 2003. A re-evaluation of long-term flux measurement techniques – Part I: averaging and coordinate rotation. Bound. Layer Meteorol. 107 (1), 1–48.

Fisher, J.B., Tu, K.P., Baldocchi, D.D., 2008. Global estimates of the land-atmosphere water flux based on monthly AVHRR and ISLSCP-II data, validated at 16 FLUXNET sites. Remote Sens. Environ. 112 (3), 901–919.

Fisher, J.B., Whittaker, R.J., Malhi, Y., 2011. ET come home: potential evapotranspiration in geographical ecology. Global Ecol. Biogeogr. 20 (1), 1–18.

Flint, A.L., Childs, S.W., 1991. Use of the Priestley-Taylor evaporation equation for soil water limited conditions in a small forest clearcut. Agric. Forest Meteorol. 56 (3–4), 247–260.

Foken, T., 2008. The energy balance closure problem: an overview. Ecol. Appl. 18 (6), 1351–1367.
Foken, T., Aubinet, M., Finnigan, J.J., Leclerc, M.Y., Mauder, M., Paw U, K.T., 2011. Results of a panel discussion about the energy balance closure correction for trace gases. Bull. Am. Meteorol. Soc. 92 (4), ES13–ES18.
Foken, T., Leuning, R., Oncley, S.R., Mauder, M., Aubinet, M., 2012. Corrections and data quality control. In: Aubinet, M., Vesala, T., Papale, D. (Eds.), Eddy Covariance. Springer, pp. 85–131.
Franssen, H.J.H., Stöckli, R., Lehner, I., Rotenberg, E., Seneviratne, S.I., 2010. Energy balance closure of eddy-covariance data: a multisite analysis for European FLUXNET stations. Agric. Forest Meteorol. 150 (12), 1553–1567.
García, M., Sandholt, I., Ceccato, P., Ridler, M., Mougin, E., Kergoat, L., Morillas, L., Timouk, F., Fensholt, R., Domingo, F., 2013. Actual evapotranspiration in drylands derived from in-situ and satellite data: assessing biophysical constraints. Remote Sens. Environ. 131 (0), 103–118.
Gibson, L.A., Münch, Z., Engelbrecht, J., 2011. Particular uncertainties encountered in using a pre-packaged SEBS model to derive evapotranspiration in a heterogeneous study area in South Africa. Hydrol. Earth Syst. Sci. 15 (1), 295–310.
Gilmanov, T.G., Soussana, J.F., Aires, L., Allard, V., Ammann, C., Balzarolo, M., Barcza, Z., Bernhofer, C., Campbell, C.L., Cernusca, A., 2007. Partitioning European grassland net ecosystem CO_2 exchange into gross primary productivity and ecosystem respiration using light response function analysis. Agric. Ecosyst. Environ. 121 (1), 93–120.
Graham, L.P., Andréasson, J., Carlsson, B., 2007. Assessing climate change impacts on hydrology from an ensemble of regional climate models, model scales and linking methods – a case study on the Lule River basin. Clim. Change 81 (1), 293–307.
Guo, Z., Dirmeyer, P.A., Gao, X., Zhao, M., 2007. Improving the quality of simulated soil moisture with a multi-model ensemble approach. Q. J. R. Meteorol. Soc. 133 (624), 731–747.
Han, S., Hu, H., Yang, D., Tian, F., 2011. A complementary relationship evaporation model referring to the Granger model and the advection–aridity model. Hydrol. Process. 25 (13), 2094–2101.
Harman, I., 2012. The role of roughness sublayer dynamics within surface exchange schemes. Bound. Layer Meteorol. 142 (1), 1–20.
Harman, I., Finnigan, J., 2007. A simple unified theory for flow in the canopy and roughness sublayer. Bound. Layer Meteorol. 123 (2), 339–363.
Haverd, V., Cuntz, M., Leuning, R., Keith, H., 2007. Air and biomass heat storage fluxes in a forest canopy: calculation within a soil vegetation atmosphere transfer model. Agric. Forest Meteorol. 147 (3–4), 125–139.
Hobbins, M.T., Ramírez, J.A., Brown, T.C., 2001. The complementary relationship in estimation of regional evapotranspiration: an enhanced advection-aridity model. Water Resour. Res. 37 (5), 1389–1403.
Hollinger, D.Y., Ollinger, S.V., Richardson, A.D., Meyers, T.P., Dail, D.B., Martin, M.E., Scott, N.A., Arkebauer, T.J., Baldocchi, D.D., Clark, K.L., 2010. Albedo estimates for land surface models and support for a new paradigm based on foliage nitrogen concentration. Glob. Change Biol. 16 (2), 696–710.
Horn, J.E., Schulz, K., 2011. Identification of a general light use efficiency model for gross primary production. Biogeosciences 8, 999–1021.
Huntington, J.L., Szilagyi, J., Tyler, S.W., Pohll, G.M., 2011. Evaluating the complementary relationship for estimating evapotranspiration from arid shrublands. Water Resour. Res. 47 (5), W05533.
Hutley, L.B., Leuning, R., Beringer, J., Cleugh, H.A., 2005. The utility of the eddy covariance techniques as a tool in carbon accounting: tropical savanna as a case study. Aust. J. Bot. 53 (7), 663–675.
Irmak, S., Haman, D.Z., 2003. Evapotranspiration: Potential or Reference. Agricultural Engineering Florida Cooperative Extension Service, Institute of Food and Agricultural Sciences, University of Florida, ABE, pp. 343.
Jacquemin, B., Noilhan, J., 1990. Sensitivity study and validation of a land surface parameterization using the HAPEX-MOBILHY data set. Bound. Layer Meteorol. 52 (1), 93–134.
Jiménez-Muñoz, J., Sobrino, J., Plaza, A., Guanter, L., Moreno, J., Martinez, P., 2009. Comparison between fractional vegetation cover retrievals from vegetation indices and spectral mixture analysis: Case Study of PROBA/CHRIS data over an agricultural area. Sensors 9 (2), 768–793.
Jiménez, C., Prigent, C., Mueller, B., Seneviratne, S.I., McCabe, M.F., Wood, E.F., Rossow, W.B., Balsamo, G., Betts, A.K., Dirmeyer, P.A., Fisher, J.B., Jung, M., Kanamitsu, M., Reichle, R.H., Reichstein, M., Rodell, M., Sheffield, J., Tu, K., Wang, K., 2011. Global intercomparison of 12 land surface heat flux estimates. J. Geophys. Res. 116 (D2), D02102.
Kalma, J., McVicar, T., McCabe, M., 2008. Estimating land surface evaporation: a review of methods using remotely sensed surface temperature data. Surv. Geophys. 29 (4), 421–469.
Katerji, N., Rana, G., Fahed, S., 2010. Parameterizing canopy resistance using mechanistic and semi-empirical estimates of hourly evapotranspiration: critical evaluation for irrigated crops in the Mediterranean. Hydrol. Process. 25 (1), 117–129.
Katul, G., Goltz, S., Hsieh, C.-I., Cheng, Y., Mowry, F., Sigmon, J., 1995. Estimation of surface heat and momentum fluxes using the flux-variance method above uniform and non-uniform terrain. Bound. Layer Meteorol. 74 (3), 237–260.
Katul, G., Hsieh, C.-I., Bowling, D., Clark, K., Shurpali, N., Turnipseed, A., Albertson, J., Tu, K., Hollinger, D., Evans, B., Offerle, B., Anderson, D., Ellsworth, D., Vogel, C., Oren, R., 1999. Spatial variability of turbulent fluxes in the roughness sublayer of an even-aged pine forest. Bound. Layer Meteorol. 93 (1), 1–28.
Kavetski, D., Kuczera, G., Franks, S.W., 2006. Bayesian analysis of input uncertainty in hydrological modeling: 1. Theory. Water Resour. Res. 42 (3), W03407.
Kracher, D., Mengelkamp, H.-T., Foken, T., 2009. The residual of the energy balance closure and its influence on the results of three SVAT models. Meteorol. Z. 18 (6), 647–661.
Kumar, A., Chen, F., Niyogi, D., Alfieri, J., Ek, M., Mitchell, K., 2011. Evaluation of a photosynthesis-based canopy resistance formulation in the Noah Land-Surface Model. Bound. Layer Meteorol. 138 (2), 263–284.
Ladson, T., Lander, J., Western, A., Grayson, R., Zhang, L., 2004. Estimating extractable soil moisture content for Australian soils. In: CRC for Catchment Hydrology.
Liu, G., Liu, Y., Hafeez, M., Xu, D., Vote, C., 2012. Comparison of two methods to derive time series of actual evapotranspiration using eddy covariance measurements in the southeastern Australia. J. Hydrol. 454–455 (0), 1–6.
Liu, Y., Zhuang, Q., Chen, M., Pan, Z., Tchebakova, N., Sokolov, A., Kicklighter, D., Melillo, J., Sirin, A., Zhou, G., He,.Y., Chen, J., Bowling, L., Miralles, D., Parfenova, E., 2013. Response of evapotranspiration and water availability to changing climate and land cover on the Mongolian Plateau during the 21st century. Global Planet. Change 108 (0), 85–99.
Lokupitiya, E., Denning, S., Paustian, K., Baker, I., Schaefer, K., Verma, S., Meyers, T., Bernacchi, C.J., Suyker, A., Fischer, M., 2009. Incorporation of crop phenology in Simple Biosphere Model (SiBcrop) to improve land-atmosphere carbon exchanges from croplands. Biogeosciences 6 (6), 969–986.
Lu, J., Sun, G., McNulty, S.G., Amatya, D.M., 2005. A comparison of six potential evapotranspiration methods for regional use in the southeastern United States. J. Am. Water Resour. Assoc. 41 (3), 621–633.
Mackay, D.S., Ewers, B.E., Loranty, M.M., Kruger, E.L., Samanta, S., 2012. Bayesian analysis of canopy transpiration models: a test of posterior parameter means against measurements. J. Hydrol. 432–433 (0), 75–83.
Mahrt, L., 2010. Computing turbulent fluxes near the surface: needed improvements. Agric. Forest Meteorol. 150 (4), 501–509.
Mahrt, L., Ek, M., 1984. The influence of atmospheric stability on potential evaporation. J. Clim. Appl. Meteorol. 23 (2), 222–234.
Massman, W.J., Lee, X., 2002. Eddy covariance flux corrections and uncertainties in long-term studies of carbon and energy exchanges. Agric. Forest Meteorol. 113 (1–4), 121–144.
Mauder, M., Foken, T., 2006. Impact of post-field data processing on eddy covariance flux estimates and energy balance closure. Meteorol. Z. 15 (6), 597–609.
Mauder, M., Foken, T., Clement, R., Elbers, J.A., Eugster, W., Grünwald, T., Heusinkveld, B., Kolle, O., 2008. Quality control of CarboEurope flux data – Part 2: Inter-comparison of eddy-covariance software. Biogeosciences 5 (2), 451–462.
McCabe, M.F., Kalma, J.D., Franks, S.W., 2005. Spatial and temporal patterns of land surface fluxes from remotely sensed surface temperatures within an uncertainty modelling framework. Hydrol. Earth Syst. Sci. 9 (5), 467–480.
McCabe, M.F., Wood, E.F., 2006. Scale influences on the remote estimation of evapotranspiration using multiple satellite sensors. Remote Sens. Environ. 105 (4), 271–285.
Miralles, D.G., Holmes, T.R.H., De Jeu, R.A.M., Gash, J.H., Meesters, A.G.C.A., Dolman, A.J., 2011. Global land-surface evaporation estimated from satellite-based observations. Hydrol. Earth Syst. Sci. 15 (2), 453–469.
Monin, A.S., Obukhov, A.M., 1945. Basic laws of turbulent mixing in the surface layer of the atmosphere. Tr. Akad. Nauk SSSR Geophiz. Inst. 24 (151), 163–187.
Monteith, J.L., 1965. Evaporation and environment. Symp. Soc. Exp. Biol. 19, 205–234.
Moriasi, D.N., Arnold, J.G., Van Liew, M.W., Bingner, R.L., Harmel, R.D., Veith, T.L., 2007. Model Evaluation Guidelines for Systematic Quantification of Accuracy in Watershed Simulations, 50. American Society of Agricultural Engineers, St. Joseph, MI, pp. 16, ETATS-UNIS.
Mu, Q., Zhao, M., Running, S.W., 2011. Improvements to a MODIS global terrestrial evapotranspiration algorithm. Remote Sens. Environ. 115 (8), 1781–1800.
Mueller, B., Hirschi, M., Jimenez, C., Ciais, P., Dirmeyer, P.A., Dolman, A.J., Fisher, J.B., Jung, M., Ludwig, F., Maignan, F., Miralles, D., McCabe, M.F., Reichstein, M., Sheffield, J., Wang, K.C., Wood, E.F., Zhang, Y., Seneviratne, S.I., 2013. Benchmark products for land evapotranspiration: LandFlux-EVAL multi-dataset synthesis. Hydrol. Earth Syst. Sci. Discuss. 10 (1), 769–805.
Mueller, B., Seneviratne, S.I., Jimenez, C., Corti, T., Hirschi, M., Balsamo, G., Ciais, P., Dirmeyer, P., Fisher, J.B., Guo, Z., Jung, M., Maignan, F., McCabe, M.F., Reichle, R., Reichstein, M., Rodell, M., Sheffield, J., Teuling, A.J., Wang, K., Wood, E.F., Zhang, Y., 2011. Evaluation of global observations-based evapotranspiration datasets and IPCC AR4 simulations. Geophys. Res. Lett. 38 (6), L06402.
Nash, J.E., Sutcliffe, J.V., 1970. River flow forecasting through conceptual models part I – a discussion of principles. J. Hydrol. 10 (3), 282–290.
Neuman, S.P., 2003. Maximum likelihood Bayesian averaging of uncertain model predictions. Stoch. Environ. Res. Risk Assess. 17 (5), 291–305.
Parlange, M.B., Katul, G.G., 1992. An advection-aridity evaporation model. Water Resour. Res. 28 (1), 127–132.
Pauwels, V.R.N., Samson, R., 2006. Comparison of different methods to measure and model actual evapotranspiration rates for a wet sloping grassland. Agric. Water Manag. 82 (1–2), 1–24.
Penman, H.L., 1948. Natural evaporation from open water, bare soil and grass. Proc. R. Soc. Lond. A. Math. Phys. Sci. 193 (1032), 120–145.
Pereira, A.R., Villa Nova, N.A., 1992. Analysis of the Priestley-Taylor parameter. Agric. Forest Meteorol. 61 (1–2), 1–9.
Priestley, C.H.B., Taylor, R.J., 1972. On the assessment of surface heat flux and evaporation using large-scale parameters. Mon. Weather Rev. 100 (2), 81–92.
Qualls, R.J., Gultekin, H., 1997. Influence of components of the advection-aridity approach on evapotranspiration estimation. J. Hydrol. 199 (1–2), 3–12.

Rana, G., Katerji, N., 2000. Measurement and estimation of actual evapotranspiration in the field under Mediterranean climate: a review. Eur. J. Agron. 13 (2–3), 125–153.
Rebmann, C., Göckede, M., Foken, T., Aubinet, M., Aurela, M., Berbigier, P., Bernhofer, C., Buchmann, N., Carrara, A., Cescatti, A., 2005. Quality analysis applied on eddy covariance measurements at complex forest sites using footprint modelling. Theor. Appl. Climatol. 80 (2–4), 121–141.
Richardson, A.D., Hollinger, D.Y., Burba, G.G., Davis, K.J., Flanagan, L.B., Katul, G.G., William, M.J., Ricciuto, D.M., Stoy, P.C., Suyker, A.E., Verma, S.B., Wofsy, S.C., 2006. A multi-site analysis of random error in tower-based measurements of carbon and energy fluxes. Agric. Forest Meteorol. 136 (1–2), 1–18.
Román, M.O., Schaaf, C.B., Woodcock, C.E., Strahler, A.H., Yang, X., Braswell, R.H., Curtis, P.S., Davis, K.J., Dragoni, D., Goulden, M.L., 2009. The MODIS (Collection V005) BRDF/albedo product: assessment of spatial representativeness over forested landscapes. Remote Sens. Environ. 113 (11), 2476–2498.
Ross, J., 1976. Radiative transfer in plant communities. In: Monteith, J.L. (Ed.), Vegetation and the Atmosphere. Academic Press, London, pp. 13–56.
Ruppert, J., Thomas, C., Foken, T., 2006. Scalar similarity for relaxed Eddy accumulation methods. Bound. Layer Meteorol. 120 (1), 39–63.
Samanta, S., Mackay, D.S., Clayton, M.K., Kruger, E.L., Ewers, B.E., 2007. Bayesian analysis for uncertainty estimation of a canopy transpiration model. Water Resour. Res. 43 (4), W04424.
Schneider, K., Ketzer, B., Breuer, L., Vaché, K.B., Bernhofer, C., Frede, H.G., 2007. Evaluation of evapotranspiration methods for model validation in a semi-arid watershed in northern China. Adv. Geosci. 11, 37–42.
Sheffield, J., Wood, E., 2008. Projected changes in drought occurrence under future global warming from multi-model, multi-scenario, IPCC AR4 simulations. Clim. Dyn. 31 (1), 79–105.
Shi, T., Guan, D., Wang, A., Wu, J., Jin, C., Han, S., 2008. Comparison of three models to estimate evapotranspiration for a temperate mixed forest. Hydrol. Process. 22 (17), 3431–3443.
Shuttleworth, W.J., Wallace, J.S., 1985. Evaporation from sparse crops-an energy combination theory. Q. J. R. Meteorol. Soc. 111 (469), 839–855.
Simpson, I.J., Thurtell, G.W., Neumann, H.H., Den Hartog, G., Edwards, G.C., 1998. The validity of similarity theory in the roughness sublayer above forests. Bound. Layer Meteorol. 87 (1), 69–99.
Sobrino, J.A., Jiménez-Muñoz, J.C., Paolini, L., 2004. Land surface temperature retrieval from LANDSAT TM 5. Remote Sens. Environ. 90 (4), 434–440.
Solano, R., Didan, K., Jacobson, A., Huete, A., 2010. MODIS Vegetation Index User's Guide Vegetation Index and Phenology Lab. The University of Arizona.
Stannard, D.I., 1993. Comparison of Penman-Monteith, Shuttleworth-Wallace, and modified Priestley-Taylor evapotranspiration models for wildland vegetation in semiarid rangeland. Water Resour. Res. 29 (5), 1379–1392.
Su, H., McCabe, M.F., Wood, E.F., Su, Z., Prueger, J.H., 2005. Modeling evapotranspiration during SMACEX: comparing two approaches for local- and regional-scale prediction. J. Hydrometeorol. 6 (6), 910–922.
Su, Z., 2002. The Surface Energy Balance System (SEBS) for estimation of turbulent heat fluxes. Hydrol. Earth Syst. Sci. 6 (1), 85–100.
Su, Z., Schmugge, T., Kustas, W.P., Massman, W.J., 2001. An evaluation of two models for estimation of the roughness height for heat transfer between the land surface and the atmosphere. J. Appl. Meteorol. 40 (11), 1933–1951.
Sulkava, M., Luyssaert, S., Zaehle, S., Papale, D., 2011. Assessing and improving the representativeness of monitoring networks: The European flux tower network example. J. Geophys. Res. 116 (G3), 2156–2202.
Sumner, D.M., Jacobs, J.M., 2005. Utility of Penman–Monteith Priestley–Taylor reference evapotranspiration, and pan evaporation methods to estimate pasture evapotranspiration. J. Hydrol. 308 (1–4), 81–104.
Tang, Q., Vivoni, E.R., Muñoz-Arriola, F., Lettenmaier, D.P., 2011. Predictability of evapotranspiration patterns using remotely sensed vegetation dynamics during the North American Monsoon. J. Hydrometeorol. 13 (1), 103–121.
Tebaldi, C., Knutti, R., 2007. The use of the multi-model ensemble in probabilistic climate projections. Philos. Trans. R. Soc. A Math. Phys. Eng. Sci. 365 (1857), 2053–2075.
Thom, A.S., 1975. Momentum, mass and heat exchange of the plant communities. In: Monteith, J.L. (Ed.), Vegetation and Atmosphere. Academic Press, London, pp. 57–109.
Timmermans, J., Su, Z., van der Tol, C., Verhoef, A., Verhoef, W., 2013. Quantifying the uncertainty in estimates of surface–atmosphere fluxes through joint evaluation of the SEBS and SCOPE models. Hydrol. Earth Syst. Sci. 17 (4), 1561–1573.
Trambouze, W., Bertuzzi, P., Voltz, M., 1998. Comparison of methods for estimating actual evapotranspiration in a row-cropped vineyard. Agric. Forest Meteorol. 91 (3–4), 193–208.
Twine, T.E., Kustas, W.P., Norman, J.M., Cook, D.R., Houser, P.R., Meyers, T.P., Prueger, J.H., Starks, P.J., Wesely, M.L., 2000. Correcting eddy-covariance flux underestimates over a grassland. Agric. Forest Meteorol. 103 (3), 279–300.
van der Kwast, J., Timmermans, W., Gieske, A., Su, Z., Olioso, A., Jia, L., Elbers, J., Karssenberg, D., de Jong, S., 2009. Evaluation of the Surface Energy Balance System (SEBS) applied to ASTER imagery with flux-measurements at the SPARC 2004 site (Barrax Spain). Hydrol. Earth Syst. Sci. 13 (7), 1337–1347.
Veenendaal, E.M., Kolle, O., Lloyd, J., 2004. Seasonal variation in energy fluxes and carbon dioxide exchange for a broad-leaved semi-arid savanna (Mopane woodland) in Southern Africa. Glob. Change Biol. 10 (3), 318–328.
Vinukollu, R.K., Meynadier, R., Sheffield, J., Wood, E.F., 2011a. Multi-model, multi-sensor estimates of global evapotranspiration: climatology, uncertainties and trends. Hydrol. Process. 25 (26), 3993–4010.
Vinukollu, R.K., Wood, E.F., Ferguson, C.R., Fisher, J.B., 2011b. Global estimates of evapotranspiration for climate studies using multi-sensor remote sensing data: evaluation of three process-based approaches. Remote Sens. Environ. 115 (3), 801–823.
Wang, K., Dickinson, R.E., 2012. A review of global terrestrial evapotranspiration: observation, modeling, climatology, and climatic variability. Rev. Geophys. 50 (2), RG2005.
Weligepolage, K., Gieske, A.S.M., van der Tol, C., Timmermans, J., Su, Z., 2012. Effect of sub-layer corrections on the roughness parameterization of a Douglas fir forest. Agric. Forest Meteorol. 162–163 (0), 115–126.
Wharton, S., Schroeder, M., Paw, U., Falk, K.T., Bible, M.K., 2009. Turbulence considerations for comparing ecosystem exchange over old-growth and clear-cut stands for limited fetch and complex canopy flow conditions. Agric. Forest Meteorol. 149 (9), 1477–1490.
Williams, M., Richardson, A.D., Reichstein, M., Stoy, P.C., Peylin, P., Verbeeck, H., Carvalhais, N., Jung, M., Hollinger, D.Y., Kattge, J., Leuning, R., Luo, Y., Tomelleri, E., Trudinger, C.M., Wang, Y.P., 2009. Improving land surface models with FLUXNET data. Biogeosciences 6 (7), 1341–1359.
Wood, E.F., Rodríguez-Iturbe, I., 1975. A Bayesian approach to analyzing uncertainty among flood frequency models. Water Resour. Res. 11 (6), 839–843.
Xiao, X., Hollinger, D., Aber, J., Goltz, M., Davidson, E.A., Zhang, Q., Moore Iii, B., 2004. Satellite-based modeling of gross primary production in an evergreen needleleaf forest. Remote Sens. Environ. 89 (4), 519–534.
Xu, C.Y., Chen, D., 2005. Comparison of seven models for estimation of evapotranspiration and groundwater recharge using lysimeter measurement data in Germany. Hydrol. Process. 19 (18), 3717–3734.
Xu, C.Y., Singh, V.P., 2002. Cross comparison of empirical equations for calculating potential evapotranspiration with data from Switzerland. Water Resour. Manag. 16 (3), 197–219.
Xystrakis, F., Matzarakis, A., 2011. Evaluation of 13 empirical reference potential evapotranspiration equations on the Island of Crete in Southern Greece. J. Irrig. Drainage Eng. 137 (4), 211–222.
Yang, H., Yang, D., Lei, Z., 2013. Seasonal variability of the complementary relationship in the Asian monsoon region. Hydrol. Process. 27 (19), 2736–2741.
Zotarelli, L., Dukes, M.D., Morgan, K.T., 2010. Interpretation of Soil Moisture Content to Determine Soil Field Capacity and Avoid Over-Irrigating Sandy Soils Using Soil Moisture Sensors.